1963

# Influence of porosity on the fracture stresses of electrical porcelain.

Edward Anton Snajdr



Department:

# INFLUENCE OF POROSITY ON THE FRACTURE STRESSES OF ELECTRICAL PORCELAIN

BY

EDWARD ANTON SNAJDR

---

A

THESIS

submitted to the faculty of the

SCHOOL OF MINES AND METALLURGY OF THE UNIVERSITY OF MISSOURI

in partial fulfillment of the requirements for the

Degree of

MASTER OF SCIENCE, CERAMIC ENGINEERING

Rolla, Missouri

1963

---

Approved by

R. E. Moore (advisor)

B. L. Atchley

William A. Frad

A. Blanje

# ABSTRACT

Spherical pores were induced in a typical quartz electrical porcelain body. Three levels of pore size and four levels of concentration were studied. Large strength sample sizes were employed using a three-point loading and diametral loading method. Data for induced quartz particles is also included.

# ACKNOWLEDGEMENTS

The author wishes to express his sincere appreciation and gratitude to Dr. R. E. Moore, Professor of Ceramic Engineering, for his help and advice during the investigation. Thanks are also due to Dr. T. J. Planje, Chairman, Ceramic Engineering Department and Prof. G. E. Lorey, Professor of Ceramic Engineering for their timely suggestions.

Illinois Edison Porcelain Company is to be commended for their cooperation in this investigation.

The author is also indebted to various members of the Metallurgical and Ceramic Departments for advice and consultation.

TABLE OF CONTENTS

# LIST OF FIGURES

# LIST OF TABLES

# CHAPTER I

## STATEMENT OF THE PROBLEM

The influence of porosity on the chemical and physical properties of materials needs a systematic approach which describes the nature of the pore size and configuration. At present many effects can be readily observed yet little is known about the mechanism of strength as a porosity dependent property. This investigation is primarily aimed at establishing a relationship between strength and a particular type of porosity condition.

The nature of the problem is such that all conditions of a strength-porosity relationship cannot be described by a single phenomenon. In this case porosity was achieved by inducing low concentrations of spherical polystyrene beads into an electrical porcelain body. The polystyrene beads burn out during firing of the body leaving a nearly spherical void. Thus the condition of porosity in this study approaches a random distribution of true spherical voids in low concentrations to minimize interactions of pores.

The evaluation of strength was done by a diametral loading and bending test. This diametral load test was employed as the primary strength test because of its adaptability to specimen fabrication and of work by a previous investigator employing this technique in a statistical strength study of electrical porcelain. The three point load was used as a comparative strength test.

The material chosen for study is a whiteware body used in the manufacture of electrical porcelain insulators. The body conforms to the requirement of statistical isotropy allowing the possibility of interpretation of the results by one or more statistical theories.(1)

# CHAPTER II

## INTRODUCTION

The effects of porosity upon the physical properties of materials may only be correctly interpreted when the nature of the porosity is adequately described. Essentially three types of porosity conditions may exist, isolated porosity, interconnecting porosity, and an intermediate type consisting of a mixture of isolated and interconnecting porosity.[2] As for the nature of the pore shape the geometrical consideration of spherical, elongated, and irregular pore types will be necessary in evaluating material properties. Irregular and elongated pores must be carefully examined to ascertain whether or not they are preferentially oriented. Pore size is also an important variable.

The previously mentioned factors affect the properties of materials simultaneously. The effects of pore size, shape, and distribution must be individually distinct from each other to produce both qualitative and quantitative results of each variable. The problem will be further complicated by the inherent properties of the materials being studied. For example a strength study of polycrystalline aluminum oxide with varying porosity will become quite complex when strength values are affected by non uniform grain sizes for varying levels of porosity.[3] In polycrystalline ceramic oxides levels of porosity are determined by the degree of sintering. Grain size will also be

determined by the sintering process. The variance of both with the sintering process will not allow a study of porosity with a constant grain size, or grain size with constant porosity. Therefore under those conditions a singular evaluation is difficult if not impossible.

Strength tests of materials have currently been under revision with emphasis placed upon the development of valid tests. Many factors will influence the test values that are not a direct result of the structure being studied. Other factors which do not reflect the properties of the microstructure such as the formulation, fabrication, processing, and testing methods used; will give varied results. It was felt that the diametral loading test had been investigated sufficiently by Moore[1] to the extent that microstructure properties could be studied with valuable results.

# CHAPTER III

# REVIEW OF LITERATURE

## A. Statistical Theories of Rupture

Manson and Smith[4] summarize Weibull's[5] work (or paper) with two main observations:

(1) Repetitive tests under similar conditions do not yield identical results, but rather a considerable dispersion of results.

(2) The mean strength as determined from a multiplicity of similar tests depends upon the volume of material stressed, the shape of the test specimen and the manner of loading i.e. tension bending and torsion etc.

Weibull's theory is an attempt to validate the hypothesis that flaws existing in materials will prevent a material from achieving its potential strength. Any dispersion of test results is due to dispersion of the flaws.

## B. General Considerations of Porosity

A general interest in the roles of porosity in various properties of materials has been stimulated by several investigators.

An example is Russell's[6] investigation which gives an approximate theory of thermal conductivity of porous materials with varing pore size and shape. He concluded that thermal conductivity is independent of pore size and

his equation depends solely upon the total porosity of the material.

Coble and Kingery[2] fabricated alumina bodies with 5 to 20% porosity by introducing crushed naphthalene into an alumina casting slip. The specimens were fired together for comparable grain development, eliminating structural variables. Effects of temperature and porosity on strength, elastic modulus of rigidity, and coefficient of thermal expansion were investigated. Effects of porosity on thermal stress resistance and torsional creep properties were studied at constant temperature.

The authors emphasize that fabricational and compositional variables had an effect on the microstructure. These variables make the evaluation of only porosity effects difficult.

In some cases corrections cannot be made for influencing variables and as a result Coble and Kingery[2] state that the qualitative agreement of porosity changes with physical properties are often completely opposite to expected results.

The shape and nature of porosity is an important feature which must be discussed in noting the strength of engineering materials. Coble and Kingery have found that when the solid phase is continuous minimum changes in physical properties are experienced. The largest changes occur when the pore phase is continuous.

Burke[7] sintered aluminum oxide powder and noted that the disappearance of pores at grain boundaries is particularly marked. Some pores disappeared while others grew larger. In some cases grain growth occurs without further densification. He concluded that the maximum densities achieved by sintering occur when grain growth is inhibited.

Seigle[8] refers to the sintering theory by Herring-Nabarro which states that voids are eliminated during the densification process of a porous mass by the migration of ions into voids from grain boundaries. In terms of vacancy migration, vacancies migrate from voids to grain boundaries. The driving force for vacancy migration is the vacancy concentration gradient, after spheroidization of the original cusped voids formed in powder compacts. If pores are close to grain boundaries densification occurs, but when grains are not close to grain boundaries densification essentially stops. Voids are preferentially eliminated at grain boundaries.

## C. Recent Strength Studies as Related to Porosity

Ryshkewitch[9] induced porosity in alumina and zirconia specimens. The specimens were prepared by forming a viscous slip of the oxide powder with water and a 0.2% solution of polyvinyl alcohol. To obtain the desired degree of porosity in the slip-cast green body, precalculated amounts of cooled slip and a 4% solution of cooled destabilized hydrogen peroxide were mixed thoroughly.

The specimens were formed by pouring the mixture into an open tray 10 x 10 cm. in area and 2 to 3 cm. thick. The slurry was then placed in a dryer at room temperature and slowly heated. The evolution of oxygen began with increasing temperature causing the slurry to expand until dry. The result was a hard strong body with fine uniformly distributed pores. This method received high praise from Duckworth.[10]

The large cakes were fired and sintered. They were then cut into cubes which were ground to give parallel faces for the strength test.

The cubes were tested in compression. The data gave a linear relationship for log strength versus porosity. In some cases elongated pores with a preferred direction of orientation of the long axis occurred. Specimens of this nature were tested with pores oriented parallel and perpendicular to the direction of loading. A ratio approximating 1.2 was found to exist between the two strength values due to orientation for bodies of the same porosity. Ryshkewitch had originally attempted to find an optimum strength as related to bulk density but finally concluded that the highest ratio of strength to specific weight occurs at the maximum specific weight.

Duckworth[10] considers Ryshkewitch's[9] experimental technique as an ingenious method of controlling porosity. He also justifies the compression test used for mechanical strength by comparing it with similar work done at Battelle Memorial Institute, Columbus, Ohio. Duckworth offers the following equation for the experimental data which is correlated with the Battelle work and that of Ryshkewitch:

$$\sigma = \sigma_o \, e^{-BP} \qquad (1)$$

$\sigma$ = Strength of porous body

$\sigma_o$ = Strength of non porous body of the same material

$P$ = Porosity expressed as a fraction = $\frac{\text{vol. of voids}}{\text{vol of specimen}}$

$B$ = Slope of the log $\sigma$ vs. P curve

For the experimental data at hand B has a value of about 7 and appears to be independent of the material. The Battelle specimens had a larger pore size than the specimens fabricated by Ryshkewitch yet the data still complies with the proposed equation. This suggests that the constant B is independent of pore size.

The following aspects were discussed by Duckworth[10] as a result of his investigation.

"1) Reduction in the cross-sectional area.

If this were the only factor, with the uniform distribution of pores that Dr. Ryshkewitch apparently achieved, the strength density ratio would not change with porosity.

2) Stress concentration factor of pores.

If this factor were significant, A smooth $\sigma$ vs. P curve would not be expected; the strength of the nonporous material would be disproportionately higher than the strengths of porous specimens.

3) Size effect.

The strength of ceramics increases with decreases in size and the small structural elements in porous bodies might be stronger than a single large element in a nonporous material. On the other hand, only a few of the small elements might be effective in bearing the load in porous specimens. In other words, the load might be more uniformly distributed in nonporous than in porous materials.

4) Prevention of crack propogation by pores.

5) Reduction in theoretical strength by the pores. Young's modulus is lowered by pores, and this may be the effective modulus that is a factor in the theoretical strength."[10]

Cutler[11] studied the effects of grain size and porosity simultaneously. The porosity was controlled by the degree of sintering. Pores of a constant size were not achieved and grain size varied throughout.

Cutler found that above the maximum temperature for densification, the strength decreases more rapidly than bulk density. The suggestion offered is that this is a result of increased void size or of increased grain size

since recrystallization occurs in this same temperature region.

In comparison to the results of Ryshkewitch[9] the dependence of strength upon porosity was so slight that a linear plot represents the data as well as the logarithmic correlation. The slopes of the lines are only one-third as much as those found by Ryshkewitch. Cutler concludes that the size of the voids makes the difference in slopes, and that the data does not distinguish between increasing crystal and void size but does indicate that strength is primarily a function of porosity.

In 1959 Knudsen[12] published an article which attempts to correlate both grain size and porosity as simultaneous factors affecting the mechanical strength of brittle polycrystalline specimens. He suggests that grain size and porosity affect ceramic materials much in the same manner as other engineering materials, namely metals. The fabrication of high strength specimens depends upon achieving the optimum balance between the decreasing porosity and increasing grain size.

A review of Balshin's work by Knudsen cites that the variation in strength of porous brittle polycrystalline specimens with changing porosity can be represented by the equation form:

$$S = So\ D^{m} \qquad (2)$$

S = Strength of a porous specimen
So= Calculated strength of a similar nonporous specimen

D = Relative Density; D = (1-porosity)
m = An empirical constant

Balshin noted in his investagations of the tensile strength of, "metal-ceramics," (presumably cermets); that the value of the constant m tended to approach a limiting value for, "optimum fabrication technology," depending upon the "characteristics" of the original powder and the time and temperature of sintering. Although his paper showed that this equation form could satisfactorily represent the relation of porosity to tensile strength of porous sintered copper powder compacts, the paper unfortunately did not contain any of his data on the "metal-ceramics," or any data illustrating the variation of the value of m. Knudsen then incorporates the work of Ryshkewitch,[9] Duwez and Martens,[13] Squire,[14] and Coble and Kingery[2] to give a correlation with Bal'shin's equation.

Duckworth's[10] equation is very similar to Bal'shin's equation if the approximation b = 1.33m is made. Knudsen's general conclusion is that equation (1) can be made to fit the data more closely than does equation (2). He has compiled the following values for b, in equation (1) from past investigations.

Ryshkewitch[9]
- Compressive strength, alumina
  - Preferential alignment of pores
    - Perpendicular to loading b = 9
    - Parallel to loading b = 8
  - Compressive strength, zirconia b = 7

Duwez and Martens[13]
- Tensile strength, steel
  - Specimens formed
    - at 40,000 lb. per sq. in. b = 7
    - at 60,000 to 100,000 lb. sq. in. b = 5

Squire[14]
Tensile strength, iron b = 5
Coble and Kingery[2]
Strength in bending, alumina b = 4

## Theoretical Considerations of Relation of Intergranular Contact Area and Specimen Porosity

Knudsen proposes that changes in porosity, as they affect strength, are deemed but indirect relative measures of changes in the critical or minimum load-bearing area within the specimen. In very porous slightly sintered specimens the critical area is not the total solid area traversed by a flat cross-sectional plane. The critical solid area is that traversed by an irregular cross-sectional surface passing between grains. This concept probably remains valid until the start of the closed pore state. Furthermore if one accepts the contention of Bal'shin that the contact between grains is weaker than the grains then the specimen strength would be dependent upon the area of contact between grains for all ranges of porosity. The structure of actual specimens is much too disordered to permit an analysis of the relation between strength, porosity, and contact area. Nevertheless if one assumes that the intergranular contact areas are weaker than the grains, one can develop an approximate concept of the relation by defining a theoretical, idealized specimen having a very orderly structure and calculating the relative increase in contact area and strength with decreasing specimen porosity.

The idealized specimen is to be composed originally of a systematic arrangement of equal sized spheres. During fabrication of the specimen: 1) The spheres draw together on their centers without changing their relative angular orientation with respect to one another. 2) Each sphere flattens at the areas of contact with its neighbors. 3) Each sphere maintains its original volume, the displaced material redistributing itself evenly over the residual curved surfaces. 4) As the porosity of the specimen decreases the size of the flattened areas of contact increases, until the original spheres eventually become polyhedrons at zero porosity.

For all types of spherical packing one may calculate the initial porosity of the specimen and the increase of the contact area between any two grains as the porosity decreases. If the intergranular contact is the weakest link within this specimen, as presupposed, then the load-bearing ability of the specimen will increase directly as the size of the contact area between two grains increases. By compensating for the associated decrease in bulk volume of the specimen one can calculate the relative increase in the strength of the specimen.

Spriggs[15] offers an expression for the elastic modulus as a function of porosity. His investigation of all data available to him can be made to fit the following expression:

$$E = E_o\, e^{-bP} \qquad (3)$$

E = Elastic modulus of porous polycrystalline specimen
$E_o$ = Elastic modulus of nonporous polycrystalline specimen
e = Napierian number 2.71828
b = Empirical constant
P = Volume fraction of porosity = $\frac{\text{void volume}}{\text{total specimen volume}}$

Spriggs investigated the mechanical properties of hot pressed magnesia and alumina with the room temperature elastic modulus being interpreted by an exponential expression of the type suggested by Knudsen[12] and Duckworth.[10]

Knudsen[16] follows Spriggs[15] paper with data which fits Spriggs[15] equation.

Hasselman[17] refers to Spriggs[15] equation and improves it by satisfying the boundary condition when P = 1. Otherwise the values of $E_o$ and b obtained from experimental data will be affected. Hasselman's equation is as follows:

$$E = E_o\left(1 + \frac{AP}{1-(A+1)P}\right) \qquad (4)$$

where

P = Pore fraction
E = Elastic modulus
$E_o$ = Elastic modulus of continuous phase
A = Constant

The equation is proposed to be more flexible than the exponential offered by Spriggs[15] as may be illustrated by the Elastic Moduli of a material containing cylindrical pores. In this example the relative decrease in Young's Modulus of Elasticity in the direction parallel to the pore, to a first approximation is equal to the volume fraction of porosity. The porosity dependence of the elastic modulus then cannot be expressed by a single equation valid over the total range of porosity from zero to unity.

Immediately following Hasselman's[17] correction Spriggs[18] suggests that better fits of data to equation (3) may be obtained by simultaneous assessment of the individual effects of open and closed pores and not the total volume fraction.

Cutler[19] relates the mechanical and physical properties of multicrystalline ceramic oxides to segregated doping elements on high purity $Al_2O_3$ and MgO bodies which where produced by new techniques. Samples were presintered with impurities of $0\text{-}10^4$ppm. The Modulus of Rupture versus grain size and densities were found. A plot for MgO is given of Modulus of Rupture versus log porosity with the doping elements held constant. The slopes of several lines are constant for different doping elements. For $Al_2O_3$ a log porosity versus Modulus of Rupture plot is offered with similar results.

# CHAPTER IV

# EXPERIMENTAL PROCEDURES

## A. Preparation of Strength Specimens

### 1. Starting materials

The body employed in this study had been previously formulated as a commercial body for the manufacture of electrical porcelain. It was received in the form of 25 to 50 pound slugs after having been blunged, filter pressed, and extruded.

Spherical polystyrene beads manufactured by the Koppers Chemical Company as 100 Dylene Fines were fractionated into three distinct particle size distributions. A first attempt at separation involved the use of an air infrasizer but static electric charges were produced by the beads and an effective separation was not accomplished. A second method attempted was by dry sieving the beads with Tyler Sieves. This method was satisfactory for eliminating large beads but as the sieve openings became smaller the separation became impossible because of sieve blinding. A successful method was developed for separation of the beads into distributions with arithmetical means of 195, 145, and 195 microns. The distributions are shown in Table I. The method developed for separation consisted merely of wet sieving the beads with alcohol. Water could not be used as a suspension medium because the beads tended to froth and as a result, floated on the liquid surface. The density of the beads is

TABLE I

FREQUENCY DISTRIBUTIONS FOR POLYSTYRENE BEADS

FROM MICROSCOPIC PARTICLE SIZE DETERMINATION

| A | | B | | C | |
|---|---|---|---|---|---|
| Diameter (microns) | f | Diameter | f | Diameter | f |
| 100-109 | 5 | 70- 79 | 1 | 40- 49 | 0 |
| 110-119 | 5 | 80- 89 | 3 | 50- 59 | 2 |
| 120-129 | 7 | 90- 99 | 3 | 60- 69 | 3 |
| 130-139 | 6 | 100-109 | 8 | 70- 79 | 10 |
| 140-149 | 10 | 110-119 | 5 | 80- 89 | 22 |
| 150-159 | 24 | 120-129 | 30 | 90- 99 | 18 |
| 160-169 | 17 | 130-139 | 32 | 100-109 | 19 |
| 170-179 | 18 | 140-149 | 57 | 110-119 | 20 |
| 180-189 | 24 | 150-159 | 42 | 120-129 | 4 |
| 190-199 | 19 | 160-169 | 48 | 130-139 | 1 |
| 200-209 | 38 | 170-179 | 26 | | |
| 210-219 | 26 | 180-189 | 11 | | |
| 220-229 | 31 | 190-199 | 5 | | |
| 230-239 | 15 | 200-209 | 1 | | |
| 240-249 | 17 | | | | |
| 250-259 | 24 | | | | |
| $\bar{x}$ = 192 Microns | | $\bar{x}$ = 148 Microns | | $\bar{x}$ = 94 Microns | |
| $\bar{x} \approx$ 195 Microns | | $\bar{x} \approx$ 145 Microns | | $\bar{x} \approx$ 95 Microns | |

about 1.06 grams per cubic centimeter. Figure 1. shows the Polystyrene beads before they were dispersed in the porcelain body.

2. Body preparation and forming method

An amount of dry body was ground from the slugs to pass a 100 mesh sieve. Beads from the A distribution (See Table I) were added to the dry body in concentrations of 1.0%, 0.5%, 0.2%, and 0.05% by weight. These additions are based upon the original weight of the dry body. These concentrations were designated as A-1, A-2, A-3, and A-4 respectively.

A separate batch of dry body was used for distributions B and C. For this reason two different control batches were made without bead additions. One batch was designated as, "A-Control," for the A distribution and another was designated as, "B and C-Control," for the B and C distributions.

The B distribution was added to dry body in the additions of 1.5%, 0.75%, 0.325%, and 0.075%, which were designated as B-1, B-2, B-3, and B-4 respectively. The C distribution was added to dry body in additions of 2.5%, 1.25%, 0.625% and 0.125%, which were designated as C-1, C-2, C-3, and C-4 respectively.

The batches were then blunged and dewatered in plaster of Paris dewatering bowls. Three-quarter-inch bars were extruded from a vacuum de-airing laboratory extruder. The column was cut into 6-inch lengths which were first air dried and then oven dried at 220$^{o}$F.

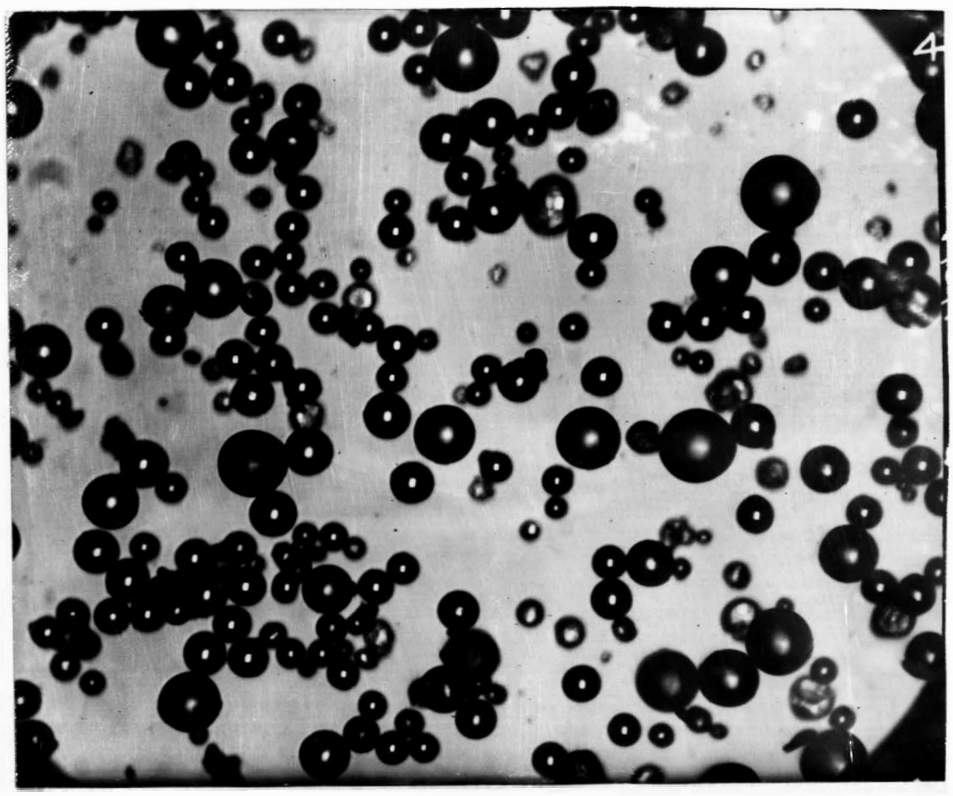

FIGURE 1. Polystyrene beads (Unfractionated) viewed under transmitted light.

3. Test specimen preparation

Specimens of all levels of bead size and at all concentrations were prepared for both the diametral loading test and the bending test.

In preparing the specimens for the strength tests in bending, one-quarter-inch holes were drilled along a diameter that was at one end of the 6-inch bars for the purpose of suspending them vertically in the furnace during firing.

The specimens of the diametral loading test were prepared by cutting the dried 6-inch bars into 1-inch lengths and facing the ends on a lathe with a carbide facing tool.

Approximately 110 specimens of each bead concentration and control batch were made for the diametral load test and 25 specimens of each were made for the bending test.

4. Firing procedure

The specimens were fired in a commercial gas fired tunnel kiln and randomized to distribute firing effects. The diametral and bending test samples were not fired simultaneously.

B. Strength Testing Procedures

1. Cross breaking method

Specimens of all concentrations and size levels were broken under three-point loading and the fracture stress S, calculated, employing the flexure formula for outer fiber stress in beams loaded at the center:

$$S = \frac{Mc}{I}$$

where:

M = small force moment
c = distance to neutral axis
I = moment of inertia

For cylindrical beams this Equation becomes:

$$S = \frac{8PL}{\pi d^3}$$

where:

P = load at center span
L = span load
d = diameter

2. Diametral loading method

P. Carneiro[20] introduced the diametrally loaded cylinder technique in 1947. This method is suited only to brittle materials in the sense that they obey Hooke's law of failure.

Due to the limitations of the direct tension and cross break bending methods the diametral cylinder method was chosen. Using this method it was felt that an optimum was reached between consistency of specimen (size, fabrication, and shape) and value of the strength test.

The cross breaking and tensile methods invariably will show fractures which are influenced by their respective gripping techniques. It is also felt that results of the cross breaking method will be affected by surface defects, because maximum stress before fracture are only achieved at outer fibers.

In 1955 Wright[21] published a study comparing strength testing methods, including the diametral loading method, for concretes. In this investigation he determined the affects of specimen dimensions with loading strip size and materials.

In 1961 Moore[1] applied the diametral loading test to the measurement of tensile strengths of electrical porcelain. This possibly was the first application of this method to brittle ceramic materials. He noted a secondary fracture surface which is attributed to compressive forces on the two halves of the specimen when the initial strain is released upon primary fracture.

Moore's conclusion is that this method has great merit when the sample supply is limited.

Rudnick, Hunter, and Holden[22] have recently completed an investigation describing the mode of fracture including photoelastic studies of padding materials at the region of applied loads and surface conditions.

The fracture mode of specimens may be of a shear type, a normal tensile type and is of primary interest and is the same as that described by Moore.[1] It was found that the triple fracture initiates along the loaded diameter causing the central break. The load causing this central break is the highest obtained during the test. The outer fracture surfaces are developed subsequent to the central crack under the influences of the remaining load. This latter investigation then establishes the validity of the triple fracture

surface with photoelastic studies of half disks with load applied at the free diameter, thus allowing the determination of tensile stresses. Here too all levels of porosity and pore size were studied by this method. The equation used for maximum tensile stresses S, developed in a cylinder at failure is:

$$S = \frac{2P}{\pi DL}$$

where:

P = applied load
D = diameter of cylinder
L = length of the cylinder

Rudnick et.al.[22] found that padding helps create a uniform stress distribution along the specimen length, reduces the magnitude of the maximum compressive and shear stresses and causes the stress acting across the loaded diameter to depart from uniform tension in the region under the applied loads.

C. Microscopic Techniques

As suggested by Moore[1] the reflected light method was employed for studying pore size and distribution. A technique for specimen preparation has been developed which shows the microstructure in great detail.

> As described by Moore,[1] "A technique for specimen preparation was developed employing a Buehler Automet grinding and polishing machine. Porcelain specimens were mounted in bakelite and ground six at a time on 200, 300, 400, and 600 grit automet abrasive paper. While in the same sample mount, they were polished on

> a low nap (Buehler Metcloth) cloth using Linde A or Linde B alumina, or 2 micron diamond abrasive. The diamond abrasive gave better results."

The polished specimens were etched with a 10% HF solution for 5-30 seconds. Overetching darkens the matrix microstructure.

For low magnification and large field areas the Unitron Metallograph was used for photomicrography. A Bausch and Lomb Research Metallograph was used at higher magnifications.

# CHAPTER V

# RESULTS AND DISCUSSION

## A. Size Distribution and Pore Shape of the Induced Porosity by Microscopic Examination

Figures 2, 3, and 4 are intended to show, size distribution differences of the induced pores for bodies A-1, B-1 and C-1 whose pore concentrations are 1.0%, 1.5% and 2.5% respectively. The representation is not a good one because the area of the field is too small to give an adequate picture of the distributions for the lower concentrations. For this reason photomicrographs were not made of concentrations less than 1%.

Size determinations were made to find the maximum pore size produced by the induced polystyrene beads. The maximum size, of the pores was equal to the maximum size of the original beads for a particular distribution giving an indication of little or no change in size of the beads when they burn out to form spherical pores, Figures 5, 6, and 7 are photomicrographs of the 195, 145, and 95 micron average pore distributions. Here some indication of size can be seen, however, these figures do not allow determination of the average pore size but rather the largest pore observed in the field .

Point count data was taken to assess induced porosity, but the measured porosity of each of the highest concentra-

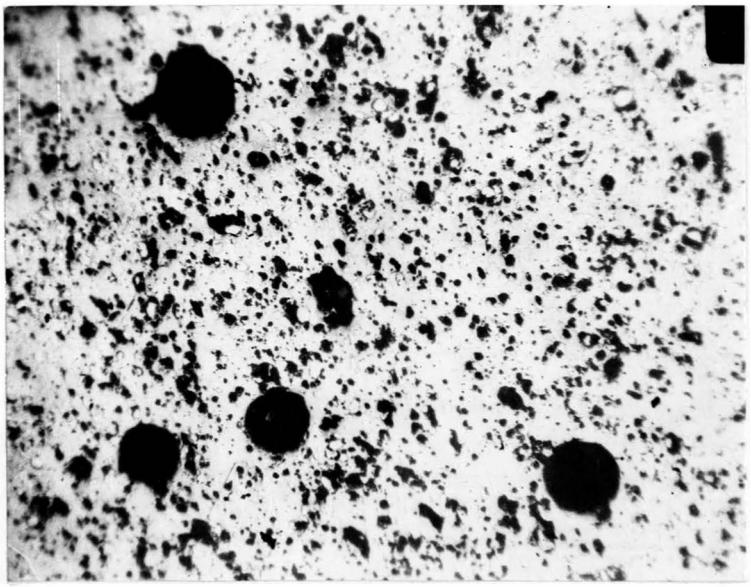

FIGURE 2. Photomicrograph of body A-1 after firing with 195 micron bead addition viewed under reflected light. 36x

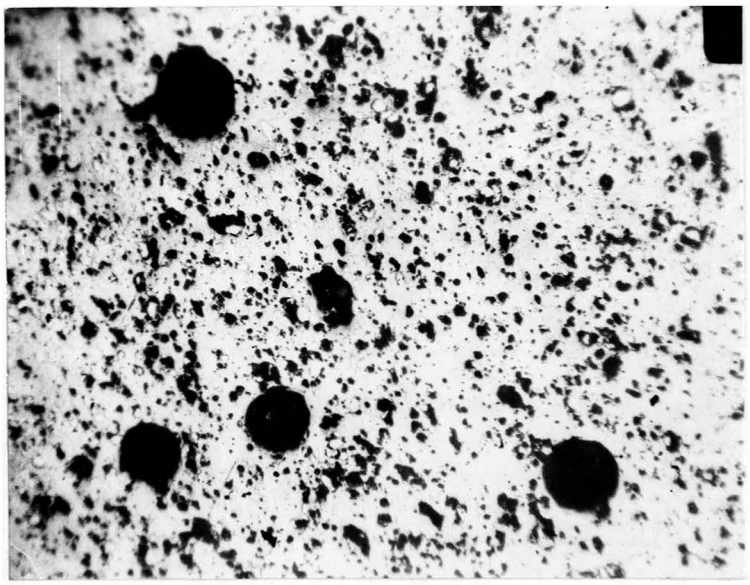

FIGURE 3. Photomicrograph of body B-1 after firing with 145 micron bead addition viewed under reflected light. 36x

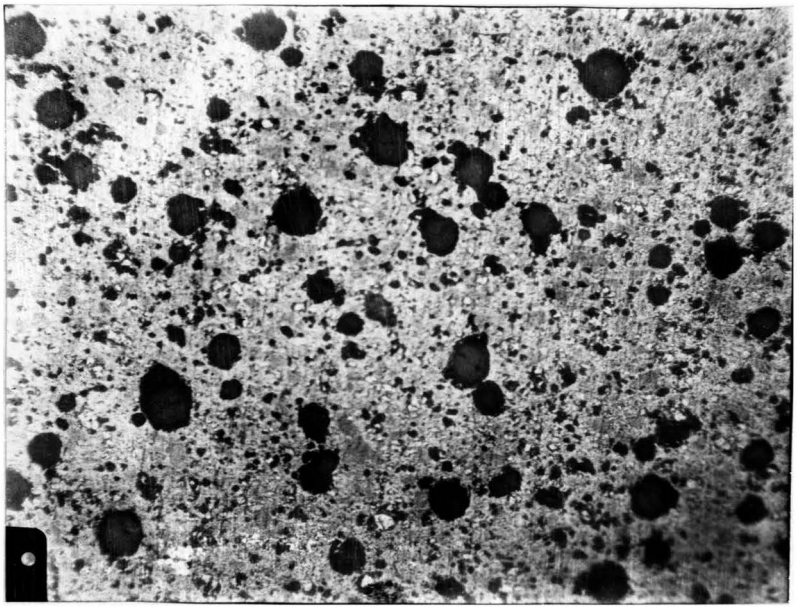

FIGURE 4. Photomicrograph of body C-1 after firing with 95 micron bead addition viewed with reflected light. 36x

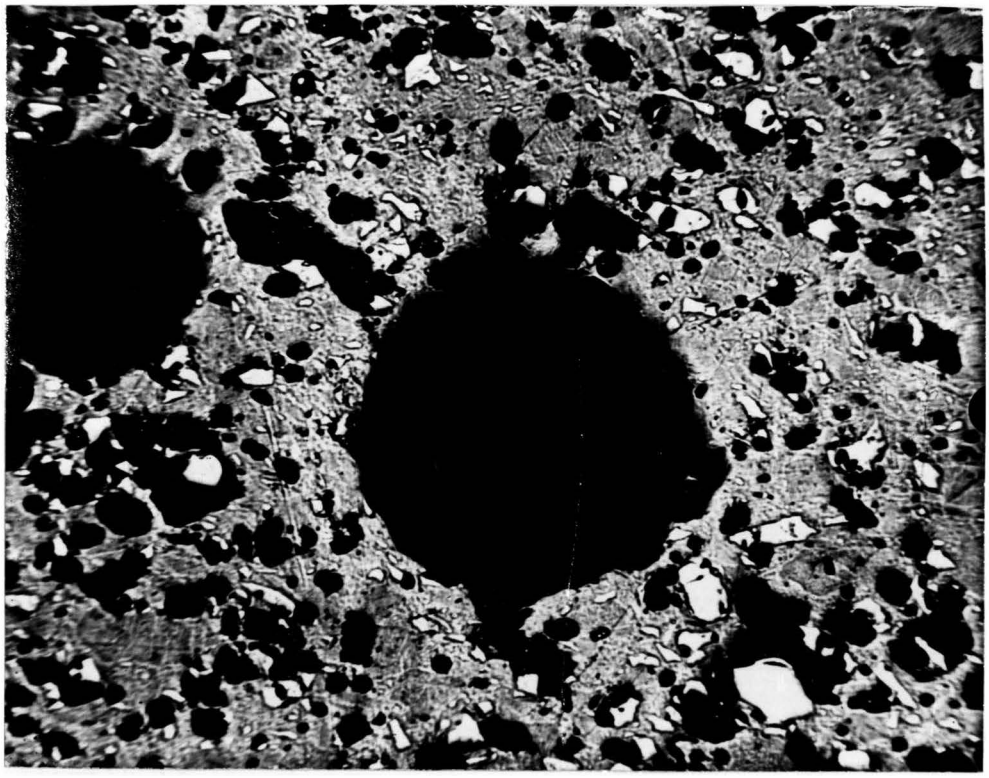

FIGURE 5. Photomicrograph of body A-1 with 195 micron beads addition after firing viewed with reflected light. 360x

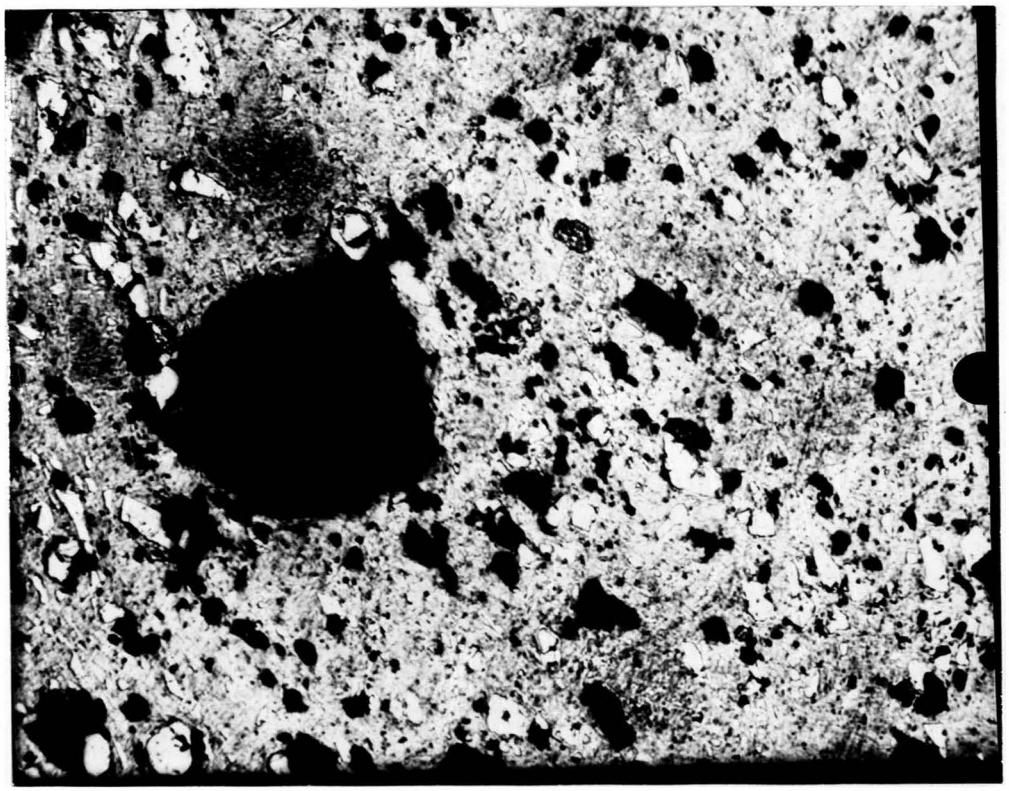

FIGURE 6. Photomicrograph of body B-1 with 145 micron bead addition viewed with reflected light. 360x

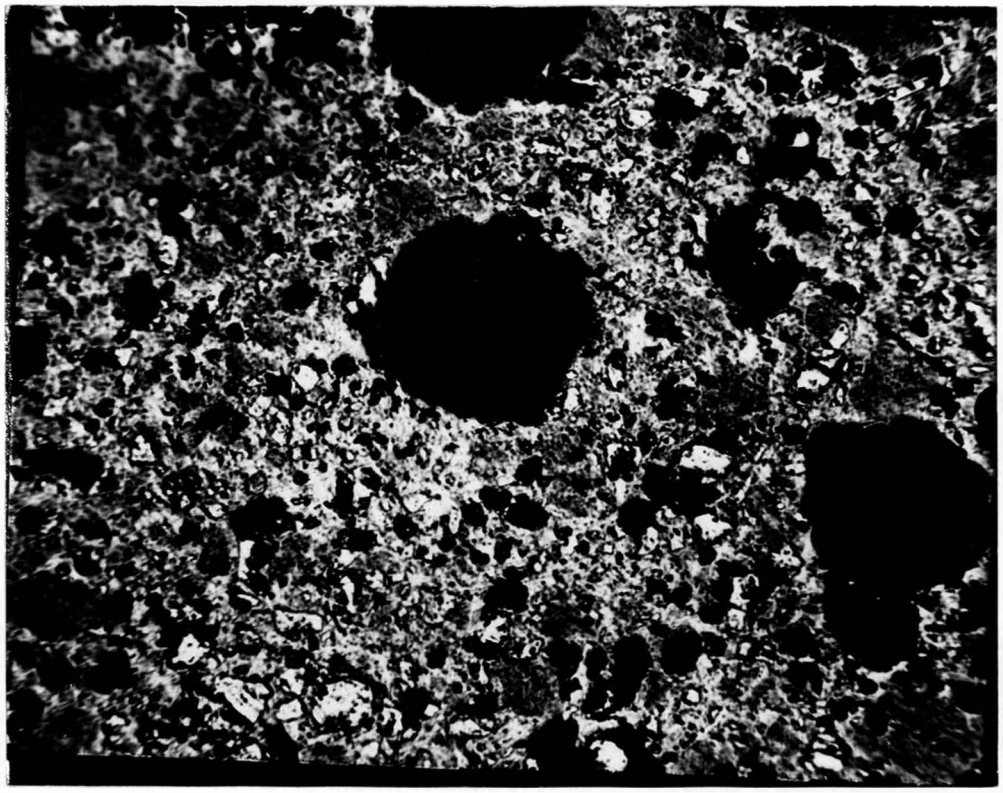

FIGURE 7. Photomicrograph of body C-1 with 95 micron bead addition viewed with reflected light. 360x

tions deviated from the calculated induced volume porosity by almost a factor of two. This error is believed to be caused by the collapse of material when a pore lies near the surface being polished and also by quartz particles which have been pulled out of the matrix during polishing appear as voids.

B. Fracture Stress as a Function of Porosity

The fired samples used for the diametral loading method were cylinders of about .650 inches in diameter and .750 inches in length. The faces (ends) of the cylinder tended to be concave due to the forming (extrusion) method.

Some values of the fracture stresses have been rejected from the unscreened data to give data which should be free of bias. Before fracture the rejection was based on observing visible defects which occurred on the surface of the specimen. After fracture the basis for rejection was the impression left on the loading pad. If the test specimen was not cylindrical in shape or the testing machine platens were not parallel the load impression would be uneven and the fracture stress was considered as not giving a valid test result.

Tables II - XV present the arithmetical mean, standard deviation, and grouped frequency distribution of the screened fracture stress data in diametral compression for all levels of pore size and concentration. These

TABLE II

GROUPED FREQUENCY DISTRIBUTION OF DIAMETRAL FRACTURE STRESSES CALCULATION OF THE MEAN AND STANDARD DEVIATION OF SAMPLE A-CONTROL SCREENED DATA

| Mid Value | f | d | fd | $fd^2$ |
|---|---|---|---|---|
| 4295 | 1 | -7 | -7 | 49 |
| 4495 | 0 | -6 | -0 | 0 |
| 4695 | 1 | -5 | -5 | 25 |
| 4895 | 2 | -4 | -8 | 32 |
| 5095 | 7 | -3 | -21 | 63 |
| 5295 | 4 | -2 | -8 | 16 |
| 5495 | 14 | -1 | -14 | 14 |
| 5695 | 12 | 0 | 0 | 0 |
| 5895 | 9 | 1 | 9 | 9 |
| 6095 | 12 | 2 | 24 | 48 |
| 6295 | 5 | 3 | 8 | 24 |
| 6495 | 3 | 4 | 12 | 48 |
| | 70 | | -10 | 328 |

$$\bar{x} = 5695 - \left(\frac{10}{70}\right)(200) = 5666 \text{ psi}$$

$$= (200)\ \frac{328 - \frac{100}{70}}{69} = 436 \text{ psi}$$

TABLE III

GROUPED FREQUENCY DISTRIBUTION OF DIAMETRAL FRACTURE STRESSES CALCULATION OF THE MEAN AND STANDARD DEVIATION OF SAMPLE A-1: 195 MICRON PORES AT 1.0% SCREENED DATA

| Mid Value | f | d | fd | $fd^2$ |
|---|---|---|---|---|
| 3095 | 2 | -7 | -14 | 98 |
| 3295 | 0 | -6 | -0 | 0 |
| 3495 | 0 | -5 | -0 | 0 |
| 3695 | 1 | -4 | -4 | 16 |
| 3895 | 4 | -3 | -12 | 36 |
| 4095 | 8 | -2 | -16 | 32 |
| 4295 | 9 | -1 | -9 | 9 |
| 4495 | 7 | 0 | 0 | 0 |
| 4695 | 4 | 1 | 4 | 4 |
| 4895 | 11 | 2 | 22 | 44 |
| 5095 | 6 | 3 | 18 | 54 |
| 5295 | 4 | 4 | 16 | 64 |
| | 56 | | +5 | 357 |

$$\bar{x} = 4495 + \left(\frac{5}{56}\right)(200) = 4513 \text{ psi}$$

$$\sigma = (200)\sqrt{\frac{357 + \frac{25}{56}}{55}} = 510 \text{ psi}$$

TABLE IV

GROUPED FREQUENCY DISTRIBUTION OF DIAMETRAL FRACTURE STRESSES CALCULATION OF THE MEAN AND STANDARD DEVIATION OF SAMPLE A-2: 195 MICRON PORES AT 0.5%

SCREENED DATA

| Mid Value | f | d | fd | $fd^2$ |
|---|---|---|---|---|
| 3895 | 3 | -4 | -12 | 48 |
| 4095 | 4 | -3 | -12 | 36 |
| 4295 | 5 | -2 | -10 | 20 |
| 4495 | 6 | -1 | -6 | 6 |
| 4695 | 7 | 0 | 0 | 0 |
| 4895 | 8 | 1 | 8 | 8 |
| 5095 | 6 | 2 | 12 | 24 |
| 5295 | 5 | 3 | 15 | 45 |
| 5495 | 2 | 4 | 8 | 32 |
| 5695 | 1 | 5 | 5 | 25 |
| | 47 | | +8 | 244 |

$$\bar{x} = 4695 + \left(\frac{8}{47}\right)(200) = 4729 \text{ psi}$$

$$\sigma = (200)\sqrt{\frac{244 - \frac{64}{47}}{46}} = 462 \text{ psi}$$

TABLE V

GROUPED FREQUENCY DISTRIBUTION OF DIAMETRAL FRACTURE STRESSES CALCULATION OF THE MEAN AND STANDARD DEVIATION OF SAMPLE A-3: 195 MICRON PORES AT 0.2% SCREENED DATA

| Mid Value | f | d | fd | $fd^2$ |
|---|---|---|---|---|
| 3295 | 1 | -9 | -9 | 81 |
| 3495 | 0 | -8 | -0 | 0 |
| 3695 | 0 | -7 | -0 | 0 |
| 3895 | 0 | -6 | -0 | 0 |
| 4095 | 2 | -5 | -10 | 56 |
| 4295 | 4 | -4 | -16 | 64 |
| 4495 | 3 | -3 | -9 | 27 |
| 4695 | 9 | -2 | -18 | 36 |
| 4895 | 5 | -1 | -5 | 5 |
| 5095 | 12 | 0 | 0 | 0 |
| 5295 | 6 | 1 | 6 | 6 |
| 5495 | 5 | 2 | 10 | 20 |
| 5695 | 8 | 3 | 24 | 72 |
| 5895 | 3 | 4 | 12 | 48 |
| 6095 | 0 | 5 | 0 | 0 |
| 6295 | 1 | 6 | 6 | 36 |
| | 59 | | -9 | 451 |

$$\bar{x} = 5095 - \left(\frac{9}{59}\right)(200) = 5064 \text{ psi}$$

$$\sigma = (200)\sqrt{\frac{451 - \frac{81}{59}}{58}} = 558 \text{ psi}$$

TABLE VI

GROUPED FREQUENCY DISTRIBUTION OF DIAMETRAL FRACTURE STRESSES CALCULATION OF THE MEAN AND STANDARD DEVIATION OF SAMPLE A-4: 195 MICRON PORES AT 0.005% SCREENED DATA

| Mid Value | f | d | fd | $fd^2$ |
|---|---|---|---|---|
| 4695 | 4 | -4 | -16 | 64 |
| 4895 | 7 | -3 | -21 | 63 |
| 5095 | 2 | -2 | -4 | 8 |
| 5295 | 3 | -1 | -3 | 3 |
| 5495 | 17 | 0 | 0 | 0 |
| 5695 | 7 | 1 | 7 | 7 |
| 5895 | 6 | 2 | 12 | 24 |
| 6095 | 4 | 3 | 12 | 36 |
| 6295 | 0 | 4 | 0 | 0 |
| 6495 | 1 | 5 | 5 | 25 |
| | 51 | | -8 | 230 |

$$\bar{x} = 5495 - \left(\frac{8}{51}\right)(200) = 5464 \text{ psi}$$

$$\sigma = (200)\sqrt{\frac{230 - \frac{64}{51}}{50}} = 428 \text{ psi}$$

TABLE VII

GROUPED FREQUENCY DISTRIBUTION OF DIAMETRAL FRACTURE STRESSES CALCULATION OF THE MEAN AND STANDARD DEVIATION OF SAMPLE B and C-CONTROL SCREENED DATA

| Mid Value | f | d | fd | $fd^2$ |
|---|---|---|---|---|
| 4695 | 2 | -4 | -8 | 32 |
| 4895 | 3 | -3 | -9 | 27 |
| 5095 | 8 | -2 | -16 | 32 |
| 5295 | 8 | -1 | -8 | 8 |
| 5495 | 13 | 0 | 0 | 0 |
| 5695 | 10 | 1 | 10 | 10 |
| 5895 | 5 | 2 | 10 | 20 |
| 6095 | 4 | 3 | 12 | 36 |
| 6295 | 1 | 4 | 4 | 16 |
| 6495 | 2 | 5 | 10 | 50 |
| | 56 | | +5 | 231 |

$$\bar{x} = 5495 + \left(\frac{5}{56}\right)(200) = 5674 \text{ psi}$$

$$\sigma = (200)\sqrt{\frac{231 - \frac{25}{56}}{55}} = 410 \text{ psi}$$

TABLE VIII

GROUPED FREQUENCY DISTRIBUTION OF DIAMETRAL FRACTURE STRESSES CALCULATION OF THE MEAN AND STANDARD DEVIATION OF SAMPLE B-1: 145 MICRON PORES AT 1.5% SCREENED DATA

| Mid Value | f | d | fd | $fd^2$ |
|---|---|---|---|---|
| 4095 | 3 | -5 | -15 | 75 |
| 4295 | 6 | -4 | -24 | 96 |
| 4495 | 8 | -3 | -24 | 72 |
| 4695 | 14 | -2 | -28 | 56 |
| 4895 | 8 | -1 | -8 | 8 |
| 5095 | 7 | 0 | 0 | 0 |
| 5295 | 5 | 1 | 5 | 5 |
| 5495 | 3 | 2 | 6 | 12 |
| 5695 | 2 | 3 | 6 | 18 |
| 5895 | 1 | 4 | 4 | 16 |
| 6095 | 0 | 5 | 0 | 0 |
| 6295 | 0 | 6 | 0 | 0 |
| 6495 | 0 | 7 | 0 | 0 |
| 6695 | 1 | 8 | 8 | 64 |
| | 58 | | -7 | 422 |

$$\bar{x} = 5095 - \left(\frac{78}{58}\right)(200) = 4853 \text{ psi}$$

$$\sigma = (200)\sqrt{\frac{422 - \frac{490}{58}}{57}} = 486 \text{ psi}$$

TABLE IX

GROUPED FREQUENCY DISTRIBUTION OF DIAMETRAL FRACTURE STRESSES CALCULATION OF THE MEAN AND STANDARD DEVIATION OF SAMPLE B-2: 145 MICRON PORES AT 0.75% SCREENED DATA

| Mid Value | f | d | fd | $fd^2$ |
|---|---|---|---|---|
| 4095 | 2 | -5 | -10 | 50 |
| 4295 | 0 | -4 | -0 | 0 |
| 4495 | 4 | -3 | -12 | 36 |
| 4695 | 8 | -2 | -16 | 32 |
| 4895 | 6 | -1 | -6 | 6 |
| 5095 | 6 | 0 | 0 | 0 |
| 5295 | 5 | 1 | 5 | 5 |
| 5495 | 6 | 2 | 12 | 24 |
| 5695 | 6 | 3 | 18 | 54 |
| 5895 | 2 | 4 | 8 | 32 |
| 6095 | 1 | 5 | 5 | 25 |
| | 45 | | +4 | 264 |

$$\bar{x} = 5095 - \left(\frac{4}{45}\right)(200) = 5077 \text{ psi}$$

$$\sigma = (200)\sqrt{\frac{264 - \frac{16}{45}}{44}} = 490 \text{ psi}$$

TABLE X

GROUPED FREQUENCY DISTRIBUTION OF DIAMETRAL FRACTURE STRESSES CALCULATION OF THE MEAN AND STANDARD DEVIATION OF SAMPLE B-3: 145 MICRON PORES AT 0.375%

SCREENED DATA

| Mid Value | f | d | fd | $fd^2$ |
|---|---|---|---|---|
| 3695 | 1 | -7 | -7 | 49 |
| 3895 | 0 | -6 | -0 | 0 |
| 4095 | 5 | -5 | -25 | 125 |
| 4295 | 4 | -4 | -16 | 64 |
| 4495 | 3 | -3 | -9 | 27 |
| 4695 | 3 | -2 | -6 | 12 |
| 4895 | 2 | -1 | -2 | 2 |
| 5095 | 11 | 0 | 0 | 0 |
| 5295 | 5 | 1 | 5 | 5 |
| 5495 | 4 | 2 | 8 | 16 |
| 5695 | 4 | 3 | 12 | 36 |
| 5895 | 5 | 4 | 20 | 80 |
| | 47 | | -20 | 416 |

$$\bar{x} = 5095 - \left(\frac{20}{47}\right)(200) = 5010 \text{ psi}$$

$$\sigma = (200)\sqrt{\frac{416 - \frac{400}{47}}{46}} = 594 \text{ psi}$$

TABLE XI

GROUPED FREQUENCY DISTRIBUTION OF DIAMETRAL FRACTURE STRESSES CALCULATION OF THE MEAN AND STANDARD DEVIATION OF SAMPLE B-4: 145 MICRON PORES AT 0.075% SCREENED DATA

| Mid Value | f | d | fd | $fd^2$ |
|---|---|---|---|---|
| 3495 | 1 | -8 | -8 | 64 |
| 3695 | 0 | -7 | -0 | 0 |
| 3895 | 1 | -6 | -6 | 36 |
| 4095 | 3 | -5 | -15 | 75 |
| 4295 | 5 | -4 | -20 | 80 |
| 4495 | 7 | -3 | -21 | 63 |
| 4695 | 7 | -2 | -14 | 28 |
| 4895 | 5 | -1 | -5 | 5 |
| 5095 | 10 | 0 | 0 | 0 |
| 5295 | 8 | 1 | 8 | 8 |
| 5495 | 13 | 2 | 26 | 52 |
| 5695 | 12 | 3 | 36 | 108 |
| 5895 | 4 | 4 | 16 | 64 |
| 6095 | 2 | 5 | 10 | 50 |
| 6295 | 3 | 6 | 18 | 108 |
| | 81 | | +25 | 741 |

$$\bar{x} = 5158 + \left(\frac{25}{81}\right)(200) = 5158 \text{ psi}$$

$$\sigma = 200\sqrt{\frac{741 - \frac{625}{81}}{80}} = 605 \text{ psi}$$

TABLE XII

GROUPED FREQUENCY DISTRIBUTION OF DIAMETRAL FRACTURE STRESSES CALCULATION OF THE MEAN AND STANDARD DEVIATION OF SAMPLE C-1: 95 MICRON PORES AT 2.5%

SCREENED DATA

| Mid Value | f | d | fd | $fd^2$ |
|---|---|---|---|---|
| 3695 | 1 | -6 | -6 | 36 |
| 3895 | 1 | -5 | -5 | 25 |
| 4095 | 5 | -4 | -20 | 80 |
| 4295 | 3 | -3 | -9 | 27 |
| 4495 | 5 | -2 | -10 | 20 |
| 4695 | 9 | -1 | -9 | 9 |
| 4895 | 8 | 0 | 0 | 0 |
| 5095 | 8 | 1 | 8 | 8 |
| 5295 | 6 | 2 | 12 | 24 |
| 5495 | 7 | 3 | 21 | 63 |
| 5695 | 11 | 4 | 44 | 176 |
| | 64 | | +26 | 468 |

$$\bar{x} = 4895 + \left(\frac{26}{64}\right)(200) = 4976 \text{ psi}$$

$$\sigma = (200)\sqrt{\frac{468 - \frac{676}{64}}{63}} = 539 \text{ psi}$$

TABLE XIII

GROUPED FREQUENCY DISTRIBUTION OF DIAMETRAL FRACTURE STRESSES CALCULATION OF THE MEAN AND STANDARD DEVIATION OF SAMPLE C-2: 95 MICRON PORES AT 1.25% SCREENED DATA

| Mid Value | f | d | fd | $fd^2$ |
|---|---|---|---|---|
| 3895 | 1 | -6 | -6 | 36 |
| 4095 | 2 | -5 | -10 | 50 |
| 4295 | 1 | -4 | -4 | 16 |
| 4495 | 4 | -3 | -12 | 36 |
| 4695 | 2 | -2 | -4 | 8 |
| 4895 | 9 | -1 | -9 | 9 |
| 5095 | 4 | 0 | 0 | 0 |
| 5295 | 7 | 1 | 7 | 7 |
| 5495 | 7 | 2 | 14 | 28 |
| 5695 | 3 | 3 | 9 | 27 |
| 5895 | 2 | 4 | 8 | 32 |
| 6095 | 1 | 5 | 5 | 25 |
| | 43 | | -2 | 274 |

$$\bar{x} = 5095 - \left(\frac{2}{43}\right)(200) = 5086 \text{ psi}$$

$$\sigma = (200)\sqrt{\frac{274 - \frac{4}{43}}{42}} = 510 \text{ psi}$$

TABLE XIV

GROUPED FREQUENCY DISTRIBUTION OF DIAMETRAL FRACTURE STRESSES CALCULATION OF THE MEAN AND STANDARD DEVIATION OF SAMPLE C-3: 95 MICRON PORES AT 0.625% SCREENED DATA

| Mid Value | f | d | fd | $fd^2$ |
|---|---|---|---|---|
| 3295 | 1 | -10 | -10 | 100 |
| 3495 | 0 | -9 | -0 | 0 |
| 3695 | 0 | -8 | -0 | 0 |
| 3895 | 0 | -7 | -0 | 0 |
| 4095 | 0 | -6 | -0 | 0 |
| 4295 | 2 | -5 | -10 | 50 |
| 4495 | 5 | -4 | -20 | 80 |
| 4695 | 2 | -3 | -6 | 18 |
| 4895 | 5 | -2 | -10 | 20 |
| 5095 | 8 | -1 | -8 | 8 |
| 5295 | 7 | 0 | 0 | 0 |
| 5495 | 9 | 1 | 9 | 9 |
| 5695 | 8 | 2 | 16 | 32 |
| 5895 | 5 | 3 | 15 | 45 |
| 6095 | 2 | 4 | 8 | 32 |
| | 52 | | -16 | 394 |

$$\bar{x} = 5295 - \left(\frac{16}{52}\right)(200) = 5233 \text{ psi}$$

$$\sigma = (200)\sqrt{\frac{394 - \frac{256}{52}}{51}} = 552 \text{ psi}$$

TABLE XV

GROUPED FREQUENCY DISTRIBUTION OF DIAMETRAL FRACTURE STRESSES CALCULATION OF THE MEAN AND STANDARD DEVIATION OF SAMPLE C-4: 95 MICRON PORES AT 0.125%

SCREENED DATA

| Mid Value | f | d | fd | $fd^2$ |
|---|---|---|---|---|
| 4095 | 1 | -7 | -7 | 49 |
| 4295 | 1 | -6 | -6 | 36 |
| 4495 | 1 | -5 | -5 | 25 |
| 4695 | 2 | -4 | -8 | 32 |
| 4895 | 8 | -3 | -24 | 72 |
| 5095 | 8 | -2 | -16 | 32 |
| 5295 | 6 | -1 | -6 | 6 |
| 5495 | 6 | 0 | 0 | 0 |
| 5695 | 9 | 1 | 9 | 9 |
| 5895 | 4 | 2 | 8 | 16 |
| 6095 | 2 | 3 | 6 | 18 |
| 6295 | 7 | 4 | 28 | 112 |
| 6495 | 4 | 5 | 20 | 100 |
| 6695 | 2 | 6 | 12 | 72 |
| | 61 | | +11 | 579 |

$$\bar{x} = 5495 + \left(\frac{11}{61}\right)(200) = 5531 \text{ psi}$$

$$\sigma = (200)\sqrt{\frac{579 - \frac{121}{61}}{62}} = 620 \text{ psi}$$

TABLE XVI

GROUPED FREQUENCY DISTRIBUTION OF DIAMETRAL FRACTURE STRESSES THE MEAN AND STANDARD DEVIATION OF SAMPLE A-CONTROL UNSCREENED DATA

| Mid Value | f | d | fd | $fd^2$ |
|---|---|---|---|---|
| 2495 | 1 | -16 | -16 | 256 |
| 2695 | 1 | -15 | -15 | 225 |
| 2895 | 2 | -14 | -28 | 392 |
| 3095 | 0 | -13 | -0 | 0 |
| 3295 | 1 | -12 | -12 | 144 |
| 3495 | 0 | -11 | -55 | 605 |
| 3695 | 2 | -10 | -20 | 200 |
| 3895 | 1 | -9 | -9 | 81 |
| 4095 | 3 | -8 | -24 | 192 |
| 4295 | 5 | -7 | -35 | 245 |
| 4495 | 5 | -6 | -30 | 180 |
| 4695 | 3 | -5 | -15 | 75 |
| 4895 | 5 | -4 | -20 | 80 |
| 5095 | 13 | -3 | -36 | 216 |
| 5295 | 8 | -2 | -16 | 32 |
| 5495 | 14 | -1 | -14 | 14 |
| 5695 | 14 | 0 | 0 | 0 |
| 5895 | 14 | 1 | 14 | 14 |
| 6095 | 13 | 2 | 36 | 72 |
| 6295 | 6 | 3 | 18 | 54 |
| 6495 | 4 | 4 | 16 | 64 |
| | 115 | | -261 | 3142 |

$\bar{x}$ = 5241 psi

$\sigma$ = 1000 psi

TABLE XVII

GROUPED FREQUENCY DISTRIBUTION OF DIAMETRAL FRACTURE STRESSES THE MEAN AND STANDARD DEVIATION OF SAMPLE A-1: 195 MICRON PORES AT 1.0% UNSCREENED DATA

| Mid Value | f | d | fd | $fd^2$ |
|---|---|---|---|---|
| 2295 | 1 | -10 | -10 | 100 |
| 2495 | 2 | -9 | -18 | 162 |
| 2695 | 2 | -8 | -16 | 128 |
| 2895 | 0 | -7 | -0 | 0 |
| 3095 | 5 | -6 | -30 | 180 |
| 3295 | 6 | -5 | -30 | 150 |
| 3495 | 7 | -4 | -28 | 112 |
| 3695 | 5 | -3 | -15 | 45 |
| 3895 | 11 | -2 | -22 | 44 |
| 4095 | 12 | -1 | -12 | 12 |
| 4295 | 15 | 0 | 0 | 0 |
| 4495 | 7 | 1 | 7 | 7 |
| 4695 | 9 | 2 | 18 | 36 |
| 4895 | 12 | 3 | 36 | 108 |
| 5095 | 7 | 4 | 28 | 112 |
| 5295 | 4 | 5 | 20 | 100 |
| | 105 | | -72 | 1296 |

$\bar{x}$ = 4158 psi

$\sigma$ = 692 psi

TABLE XVIII

GROUPED FREQUENCY DISTRIBUTION OF DIAMETRAL FRACTURE STRESSES THE MEAN AND STANDARD DEVIATION OF SAMPLE A-2: 195 MICRON PORES AT 0.5% UNSCREENED DATA

| Mid Value | f | d | fd | $fd^2$ |
|---|---|---|---|---|
| 2895 | 3 | -7 | -21 | 147 |
| 3095 | 2 | -6 | -12 | 72 |
| 3295 | 5 | -5 | -25 | 125 |
| 3495 | 6 | -4 | -24 | 96 |
| 3695 | 4 | -3 | -12 | 36 |
| 3895 | 15 | -2 | -30 | 60 |
| 4095 | 15 | -1 | -15 | 15 |
| 4295 | 8 | 0 | 0 | 0 |
| 4495 | 9 | 1 | 9 | 9 |
| 4695 | 13 | 2 | 26 | 58 |
| 4895 | 9 | 3 | 27 | 81 |
| 5095 | 7 | 4 | 28 | 112 |
| 5295 | 6 | 5 | 30 | 150 |
| 5495 | 3 | 6 | 18 | 108 |
| 5695 | 2 | 7 | 14 | 98 |
| | 107 | | +13 | 1161 |

$\bar{x}$ = 4319 psi

$\sigma$ = 658 psi

TABLE XIX

GROUPED FREQUENCY DISTRIBUTION OF DIAMETRAL FRACTURE STRESSES THE MEAN AND STANDARD DEVIATION OF SAMPLE A-3: 195 MICRON PORES AT 0.2%

UNSCREENED DATA

| Mid Value | f | d | fd | $fd^2$ |
|---|---|---|---|---|
| 2295 | 1 | -12 | -12 | 144 |
| 2495 | 1 | -11 | -11 | 121 |
| 2695 | 3 | -10 | -30 | 300 |
| 2895 | 0 | -9 | 0 | 0 |
| 3095 | 3 | -8 | -24 | 192 |
| 3295 | 6 | -7 | -42 | 294 |
| 3495 | 8 | -6 | -48 | 288 |
| 3695 | 2 | -5 | -10 | 50 |
| 3895 | 1 | -4 | -4 | 16 |
| 4095 | 8 | -3 | -24 | 72 |
| 4295 | 10 | -2 | -20 | 40 |
| 4495 | 11 | -1 | -11 | 11 |
| 4695 | 9 | 0 | 0 | 0 |
| 4895 | 6 | 1 | 6 | 6 |
| 5095 | 15 | 2 | 30 | 60 |
| 5295 | 8 | 3 | 24 | 72 |
| 5495 | 6 | 4 | 24 | 96 |
| 5695 | 10 | 5 | 50 | 250 |
| 5895 | 3 | 6 | 18 | 108 |
| 6095 | 0 | 7 | 0 | 0 |
| 6295 | 1 | 8 | 8 | 64 |
| | 112 | | -76 | 2184 |

$\bar{x}$ = 4559 psi

$\sigma$ = 878 psi

TABLE XX

GROUPED FREQUENCY DISTRIBUTION OF DIAMETRAL FRACTURE STRESSES THE MEAN AND STANDARD DEVIATION OF SAMPLE A-4: 195 MICRON PORES AT 0.05%

UNSCREENED DATA

| Mid Value | f | d | fd | $fd^2$ |
|---|---|---|---|---|
| 2895 | 1 | -12 | -12 | 144 |
| 3095 | 0 | -11 | -0 | 0 |
| 3295 | 1 | -10 | -10 | 100 |
| 3495 | 0 | -9 | -0 | 0 |
| 3695 | 1 | -8 | -8 | 64 |
| 3895 | 4 | -7 | -28 | 196 |
| 4095 | 3 | -6 | -18 | 108 |
| 4295 | 0 | -5 | -0 | 0 |
| 4495 | 2 | -4 | -8 | 32 |
| 4695 | 8 | -3 | -24 | 72 |
| 4895 | 10 | -2 | -20 | 40 |
| 5095 | 7 | -1 | -7 | 7 |
| 5295 | 7 | 0 | 0 | 0 |
| 5495 | 20 | 1 | 20 | 20 |
| 5695 | 9 | 2 | 18 | 36 |
| 5895 | 8 | 3 | 24 | 72 |
| 6095 | 6 | 4 | 24 | 96 |
| 6295 | 0 | 5 | 0 | 0 |
| 6495 | 2 | 6 | 12 | 72 |
| 6695 | 1 | 7 | 7 | 49 |
| | 90 | | -30 | 1108 |

$\bar{x}$ = 5235 psi

$\sigma$ = 702 psi

TABLE XXI

GROUPED FREQUENCY DISTRIBUTION OF DIAMETRAL FRACTURE STRESSES THE MEAN AND STANDARD DEVIATION OF SAMPLE B and C-CONTROL UNSCREENED DATA

| Mid Value | f | d | fd | $fd^2$ |
|---|---|---|---|---|
| 3495 | 5 | -8 | -40 | 320 |
| 3695 | 4 | -7 | -28 | 196 |
| 3895 | 5 | -6 | -30 | 180 |
| 4095 | 7 | -5 | -35 | 175 |
| 4295 | 7 | -4 | -28 | 112 |
| 4495 | 7 | -3 | -21 | 63 |
| 4695 | 3 | -2 | -6 | 12 |
| 4895 | 7 | -1 | -7 | 7 |
| 5095 | 13 | 0 | 0 | 0 |
| 5295 | 8 | 11 | 8 | 8 |
| 5495 | 15 | 2 | 30 | 60 |
| 5695 | 10 | 3 | 30 | 90 |
| 5895 | 6 | 4 | 24 | 96 |
| 6095 | 6 | 5 | 30 | 150 |
| 6295 | 1 | 6 | 6 | 36 |
| 6495 | 2 | 7 | 14 | 98 |
| 6695 | 1 | 8 | 8 | 64 |
| | 107 | | -45 | 1667 |

$\bar{x}$ = 5011 psi

$\sigma$ = 788 psi

TABLE XXII

GROUPED FREQUENCY DISTRIBUTION OF DIAMETRAL FRACTURE STRESSES THE MEAN AND STANDARD DEVIATION OF SAMPLE B-1: 145 MICRON PORES AT 1.5% UNSCREENED DATA

| Mid Value | f | d | fd | $fd^2$ |
|---|---|---|---|---|
| 3095 | 1 | -8 | -8 | 64 |
| 3295 | 3 | -7 | -21 | 147 |
| 3495 | 0 | -6 | -0 | 0 |
| 3695 | 1 | -5 | -5 | 25 |
| 3895 | 7 | -4 | -28 | 112 |
| 4095 | 9 | -3 | -27 | 81 |
| 4295 | 17 | -2 | -34 | 68 |
| 4495 | 9 | -1 | -9 | 9 |
| 4695 | 15 | 0 | 0 | 0 |
| 4895 | 13 | 1 | 13 | 13 |
| 5095 | 13 | 2 | 26 | 52 |
| 5295 | 6 | 3 | 18 | 54 |
| 5495 | 4 | 4 | 16 | 64 |
| 5695 | 5 | 5 | 25 | 125 |
| 5895 | 1 | 6 | 6 | 36 |
| 6095 | 0 | 7 | 0 | 0 |
| 6295 | 0 | 8 | 0 | 0 |
| 6495 | 0 | 9 | 0 | 0 |
| 6695 | 1 | 10 | 10 | 100 |
| | 105 | | -18 | 950 |

$\bar{x}$ = 4661 psi

$\sigma$ = 604 psi

TABLE XXIII

GROUPED FREQUENCY DISTRIBUTION OF DIAMETRAL FRACTURE STRESSES THE MEAN AND STANDARD DEVIATION OF SAMPLE B-2: 145 MICRON PORES AT 0.75%

UNSCREENED DATA

| Mid Value | f | d | fd | $fd^2$ |
|---|---|---|---|---|
| 2895 | 3 | -8 | -24 | 192 |
| 3095 | 1 | -7 | -7 | 49 |
| 3295 | 5 | -6 | -30 | 180 |
| 3495 | 8 | -5 | -40 | 200 |
| 3695 | 4 | -4 | -16 | 64 |
| 3895 | 2 | -3 | -6 | 18 |
| 4095 | 16 | -2 | -32 | 64 |
| 4295 | 5 | -1 | -5 | 5 |
| 4495 | 14 | 0 | 0 | 0 |
| 4695 | 11 | 1 | 11 | 11 |
| 4895 | 6 | 2 | 12 | 24 |
| 5095 | 8 | 3 | 24 | 72 |
| 5295 | 6 | 4 | 24 | 96 |
| 5495 | 6 | 5 | 30 | 150 |
| 5695 | 6 | 6 | 36 | 216 |
| 5895 | 2 | 7 | 14 | 98 |
| 6095 | 1 | 8 | 8 | 64 |
| | 104 | | -1 | 1503 |

$\bar{x}$ = 4493 psi

$\sigma$ = 762 psi

TABLE XXIV

GROUPED FREQUENCY DISTRIBUTION OF DIAMETRAL FRACTURE STRESSES THE MEAN AND STANDARD DEVIATION OF SAMPLE B-3: 145 MICRON PORES AT 0.375% UNSCREENED DATA

| Mid Value | f | d | fd | $fd^2$ |
|---|---|---|---|---|
| 2895 | 2 | -8 | -16 | 138 |
| 3095 | 0 | -7 | -0 | 0 |
| 3295 | 5 | -6 | -30 | 180 |
| 3495 | 5 | -5 | -25 | 125 |
| 3695 | 6 | -4 | -24 | 96 |
| 3895 | 5 | -3 | -15 | 45 |
| 4095 | 8 | -2 | -16 | 32 |
| 4295 | 9 | -1 | -9 | 9 |
| 4495 | 6 | 0 | 0 | 0 |
| 4695 | 8 | 1 | 8 | 8 |
| 4895 | 7 | 2 | 14 | 28 |
| 5095 | 11 | 3 | 33 | 99 |
| 5295 | 5 | 4 | 20 | 80 |
| 5495 | 5 | 5 | 25 | 125 |
| 5695 | 4 | 6 | 24 | 144 |
| 5895 | 5 | 7 | 35 | 245 |
| | 91 | | +24 | 1354 |

$\bar{x}$ = 4548 psi

$\sigma$ = 774 psi

TABLE XXV

GROUPED FREQUENCY DISTRIBUTION OF DIAMETRAL FRACTURE STRESSES THE MEAN AND STANDARD DEVIATION OF SAMPLE B-4: 145 MICRON PORES AT 0.075%

UNSCREENED DATA

| Mid Value | f | d | fd | $fd^2$ |
|---|---|---|---|---|
| 2895 | 2 | -11 | -22 | 242 |
| 3095 | 2 | -10 | -20 | 200 |
| 3295 | 4 | -9 | -36 | 324 |
| 3495 | 1 | -8 | -8 | 64 |
| 3695 | 0 | -7 | -0 | 0 |
| 3895 | 1 | -6 | -6 | 36 |
| 4095 | 3 | -5 | -15 | 75 |
| 4295 | 5 | -4 | -20 | 80 |
| 4495 | 7 | -3 | -21 | 63 |
| 4695 | 7 | -2 | -14 | 28 |
| 4895 | 5 | -1 | -5 | 5 |
| 5095 | 10 | 0 | 0 | 0 |
| 5295 | 8 | 1 | 8 | 8 |
| 5495 | 13 | 2 | 26 | 52 |
| 5695 | 12 | 3 | 36 | 108 |
| 5895 | 4 | 4 | 16 | 64 |
| 6095 | 2 | 5 | 10 | 50 |
| 6295 | 3 | 6 | 18 | 108 |
| | 89 | | -53 | 1507 |

$\bar{x}$ = 4976 psi

$\sigma$ = 820 psi

TABLE XXVI

GROUPED FREQUENCY DISTRIBUTION OF DIAMETRAL FRACTURE STRESSES THE MEAN AND STANDARD DEVIATION OF SAMPLE C-1: 95 MICRON PORES AT 2.5% UNSCREENED DATA

| Mid Value | f | d | fd | $fd^2$ |
|---|---|---|---|---|
| 3295 | 1 | -6 | -6 | 36 |
| 3495 | 2 | -5 | -10 | 50 |
| 3695 | 3 | -4 | -12 | 48 |
| 3895 | 6 | -3 | -18 | 54 |
| 4095 | 13 | -2 | -26 | 52 |
| 4295 | 9 | -1 | -9 | 9 |
| 4495 | 8 | 0 | 0 | 0 |
| 4695 | 15 | 1 | 15 | 15 |
| 4895 | 11 | 2 | 22 | 44 |
| 5095 | 9 | 3 | 27 | 71 |
| 5295 | 6 | 4 | 24 | 96 |
| 5495 | 8 | 5 | 40 | 200 |
| 5695 | 2 | 6 | 12 | 72 |
| | 93 | | +59 | 747 |

$\bar{x}$ = 4622 psi

$\sigma$ = 556 psi

TABLE XXVII

GROUPED FREQUENCY DISTRIBUTION OF DIAMETRAL FRACTURE STRESSES THE MEAN AND STANDARD DEVIATION OF SAMPLE C-2: 95 MICRON PORES AT 1.25% UNSCREENED DATA

| Mid Value | f | d | fd | $fd^2$ |
|---|---|---|---|---|
| 3495 | 1 | -7 | -7 | 49 |
| 3695 | 5 | -6 | -30 | 180 |
| 3895 | 3 | -5 | -15 | 75 |
| 4095 | 9 | -4 | -36 | 144 |
| 4295 | 4 | -3 | -12 | 36 |
| 4495 | 9 | -2 | -18 | 36 |
| 4695 | 5 | -1 | -5 | 5 |
| 4895 | 18 | 0 | 0 | 0 |
| 5095 | 5 | 1 | 5 | 5 |
| 5295 | 3 | 2 | 6 | 12 |
| 5495 | 11 | 3 | 33 | 99 |
| 5695 | 4 | 4 | 16 | 64 |
| 5895 | 2 | 5 | 10 | 50 |
| 6095 | 11 | 6 | 66 | 396 |
| | 90 | | +13 | 1151 |

$\bar{x}$ = 4866 psi

$\sigma$ = 718 psi

TABLE XXVIII

GROUPED FREQUENCY DISTRIBUTION OF DIAMETRAL FRACTURE STRESSES THE MEAN AND STANDARD DEVIATION OF

SAMPLE C-3: 95 MICRON PORES AT 0.625%

UNSCREENED DATA

| Mid Value | f | d | fd | $fd^2$ |
|---|---|---|---|---|
| 2295 | 1 | -11 | -11 | 121 |
| 3095 | 1 | -10 | -10 | 200 |
| 3295 | 1 | -9 | -9 | 81 |
| 3495 | 1 | -8 | -8 | 64 |
| 3695 | 2 | -7 | -14 | 98 |
| 3895 | 2 | -6 | -12 | 96 |
| 4095 | 5 | -5 | -25 | 125 |
| 4295 | 6 | -4 | -10 | 40 |
| 4495 | 10 | -3 | -30 | 90 |
| 4695 | 15 | -2 | -30 | 60 |
| 4895 | 11 | -1 | -11 | 11 |
| 5095 | 8 | 0 | 0 | 0 |
| 5295 | 11 | 1 | 11 | 11 |
| 5495 | 10 | 2 | 20 | 40 |
| 5695 | 13 | 3 | 39 | 117 |
| 5895 | 9 | 4 | 36 | 144 |
| 6095 | 5 | 5 | 25 | 125 |
| 6295 | 1 | 6 | 6 | 36 |
| | 112 | | -37 | 1459 |

$\bar{x}$ = 5029 psi

$\sigma$ = 720 psi

TABLE XXIX

GROUPED FREQUENCY DISTRIBUTION OF DIAMETRAL FRACTURE STRESSES THE MEAN AND STANDARD DEVIATION OF SAMPLE C-4: 95 MICRON PORES AT 0.125% UNSCREENED DATA

| Mid Value | f | d | fd | $fd^2$ |
|---|---|---|---|---|
| 2295 | 1 | -15 | -15 | 225 |
| 2495 | 0 | -14 | -0 | 0 |
| 2695 | 0 | -13 | -0 | 0 |
| 2895 | 1 | -12 | -12 | 144 |
| 3095 | 0 | -11 | -0 | 0 |
| 3295 | 0 | -10 | -0 | 0 |
| 3495 | 2 | -9 | -18 | 162 |
| 3695 | 2 | -8 | -16 | 128 |
| 3895 | 1 | -7 | -7 | 49 |
| 4095 | 5 | -6 | -30 | 180 |
| 4295 | 4 | -5 | -20 | 100 |
| 4495 | 4 | -4 | -16 | 64 |
| 4695 | 7 | -3 | -21 | 63 |
| 4895 | 14 | -2 | -28 | 56 |
| 5095 | 11 | -1 | -11 | 11 |
| 5295 | 8 | 0 | 0 | 0 |
| 5495 | 12 | 1 | 12 | 12 |
| 5695 | 10 | 2 | 20 | 40 |
| 5895 | 6 | 3 | 18 | 54 |
| 6095 | 3 | 4 | 12 | 48 |
| 6295 | 10 | 5 | 50 | 250 |
| 6495 | 6 | 6 | 36 | 216 |
| 6695 | 3 | 7 | 21 | 147 |
| | 110 | | -25 | 1949 |

$\bar{x}$ = 5245 psi

$\sigma$ = 846 psi

TABLE XXX

FRACTURE STRESSES IN BENDING FOR 195 MICRON PORES

| A-CONTROL | | A-1 | | A-2 | | A-3 | | A-4 | |
|---|---|---|---|---|---|---|---|---|---|
| Stress | f | Stress | f | Stress | f | Stress | f | Stress | f |
| 7400 | 1 | 5700 | 3 | 5700 | 1 | 6800 | 4 | 6800 | 1 |
| 7500 | 3 | 5800 | 4 | 5800 | 0 | 6900 | 4 | 6900 | 0 |
| 7600 | 3 | 5900 | 1 | 5900 | 1 | 7000 | 1 | 7000 | 2 |
| 7700 | 5 | 6000 | 2 | 6000 | 2 | 7100 | 2 | 7100 | 0 |
| 7800 | 2 | 6100 | 1 | 6100 | 3 | 7200 | 1 | 7200 | 1 |
| 7900 | 4 | 6200 | 4 | 6200 | 3 | 7300 | 5 | 7300 | 3 |
| 8000 | 1 | 6300 | 4 | 6300 | 2 | 7400 | 0 | 7400 | 0 |
| 8100 | 3 | 6400 | 1 | 6400 | 2 | 7500 | 6 | 7500 | 4 |
| 8200 | 1 | | | 6500 | 1 | 7600 | 3 | 7600 | 1 |
| 8300 | 1 | | | 6600 | 1 | 7700 | 2 | 7700 | 3 |
| | | | | 6700 | 2 | 7800 | 1 | 7800 | 3 |
| | | | | 6800 | 1 | 7900 | 1 | 7900 | 2 |
| | | | | 6900 | 0 | 8000 | 1 | 8000 | 2 |
| | | | | 7000 | 0 | 8100 | 1 | 8100 | 5 |
| | | | | 7100 | 0 | 8200 | 0 | 8200 | 3 |
| | | | | 7200 | 1 | 8300 | 0 | 8300 | 1 |
| | | | | | | 8400 | 1 | 8400 | 2 |
| | | | | | | 8500 | 1 | 8500 | 2 |
| $\bar{x}$ = 7800 | | $\bar{x}$ = 6035 | | $\bar{x}$ = 6320 | | $\bar{x}$ = 7400 | | $\bar{x}$ = 7772 | |

TABLE XXXI

FRACTURE STRESSES IN BENDING FOR 145 MICRON PORES

| B&C CONTROL | | B-1 | | B-2 | | B-3 | | B-4 | |
|---|---|---|---|---|---|---|---|---|---|
| Stress | f | Stress | f | Stress | f | Stress | f | Stress | f |
| 7700 | 2 | 6600 | 1 | 6700 | 1 | 6900 | 2 | 7300 | 1 |
| 7800 | 1 | 6700 | 0 | 6800 | 1 | 7000 | 0 | 7400 | 2 |
| 7900 | 3 | 6800 | 0 | 6900 | 0 | 7100 | 0 | 7500 | 3 |
| 8000 | 1 | 6900 | 0 | 7000 | 2 | 7200 | 1 | 7600 | 2 |
| 8100 | 1 | 7000 | 1 | 7100 | 1 | 7300 | 3 | 7700 | 0 |
| 8200 | 5 | 7100 | 2 | 7200 | 8 | 7400 | 4 | 7800 | 4 |
| 8300 | 0 | 7200 | 1 | 7300 | 3 | 7500 | 5 | 7900 | 6 |
| 8400 | 4 | 7300 | 1 | 7400 | 3 | 7600 | 3 | 8000 | 4 |
| 8500 | 1 | 7400 | 2 | 7500 | 1 | 7700 | 5 | 8100 | 0 |
| 8600 | 4 | 7500 | 1 | 7600 | 4 | 7800 | 4 | 8200 | 3 |
| 8700 | 0 | 7600 | 1 | 7700 | 7 | 7900 | 0 | 8300 | 0 |
| 8800 | 3 | | | 7800 | 2 | 8000 | 7 | 8400 | 2 |
| | | | | 7900 | 1 | 8100 | 1 | 8500 | 1 |
| | | | | 8000 | 1 | 8200 | 4 | | |
| | | | | 8100 | 0 | 8300 | 0 | | |
| | | | | 8200 | 1 | 8400 | 0 | | |
| | | | | 8300 | 1 | 8500 | 1 | | |
| $\bar{x}$ = 8276 psi | | $\bar{x}$ = 7192 psi | | $\bar{x}$ = 7462 psi | | $\bar{x}$ = 7697 psi | | $\bar{x}$ = 7860 psi | |

TABLE XXXII

FRACTURE STRESSES IN BENDING FOR 95 MICRON PORES

| C-1 | | C-2 | | C-3 | | C-4 | |
|---|---|---|---|---|---|---|---|
| Stress | f | Stress | f | Stress | f | Stress | f |
| 6800 | 1 | 6800 | 1 | 7500 | 2 | 7300 | 1 |
| 6900 | 0 | 6900 | 0 | 7600 | 2 | 7400 | 0 |
| 7000 | 0 | 7000 | 1 | 7700 | 4 | 7500 | 0 |
| 7100 | 3 | 7100 | 1 | 7800 | 0 | 7600 | 3 |
| 7200 | 1 | 7200 | 0 | 7900 | 0 | 7700 | 3 |
| 7300 | 3 | 7300 | 3 | 8000 | 4 | 7800 | 1 |
| | | 7400 | 0 | 8100 | 3 | 7900 | 1 |
| | | 7500 | 2 | 8200 | 1 | 8000 | 7 |
| | | 7600 | 4 | 8300 | 0 | 8100 | 0 |
| | | 7700 | 3 | 8400 | 0 | 8200 | 6 |
| | | 7800 | 2 | 8500 | 1 | 8300 | 3 |
| | | 7900 | 2 | | | 8400 | 2 |
| | | 8000 | 3 | | | 8500 | 3 |
| | | 8100 | 1 | | | 8600 | 3 |
| | | 8200 | 2 | | | | |
| | | 8300 | 1 | | | | |
| $\bar{x}$ = 7222 psi | | $\bar{x}$ = 7673 psi | | $\bar{x}$ = 7882 psi | | $\bar{x}$ = 8133 psi | |

arithmetical means were plotted versusppercent volume induced porosity with linear coordinates as shown in Figure 8. The result suggests an exponential relationship for the mean fracture stress versus volume porosity. For unknown reasons the B data for the 145 micron spheres showed only a random scatter of strength versus porosity and therefore is not included in the plot. Figure 9 shows a linear plot of log volume porosity versus the mean fracture stress for the screened data. The unscreened data listed in Tables XVI - XXIX was plotted in Figure 10 in the manner previously described. The slopes of the screened data and unscreened data are identical. The only effect of including the biased data is to decrease the mean fracture stresses by about 200 to 400 psi. Fracture stresses were also determined in bending for comparison with diametral loading data. The fracture stress results of the bending test listed in Tables XXX - XXXII are shown in Figure 11. with Modulus of Rupture versus percent porosity on cartesian coordinates. The specimen diameter was approximately 0.650 inches and the length was 6 inches. The distance between the end supports of the three point load test was 4.05 inches.

The Modulus of Rupture versus porosity plot for the 95 micron size is nearly linear. This suggests that the bending test is not as sensitive to smaller size dicontinuities or flaws as is the diametral loading test which shows the exponential relationship for all bead sizes. This fact may

INDUCED SPHERICAL CLOSED PORE POROSITY
VS.
TENSILE STRENGTH IN DIAMETRAL LOADING
(SCREENED DATA)

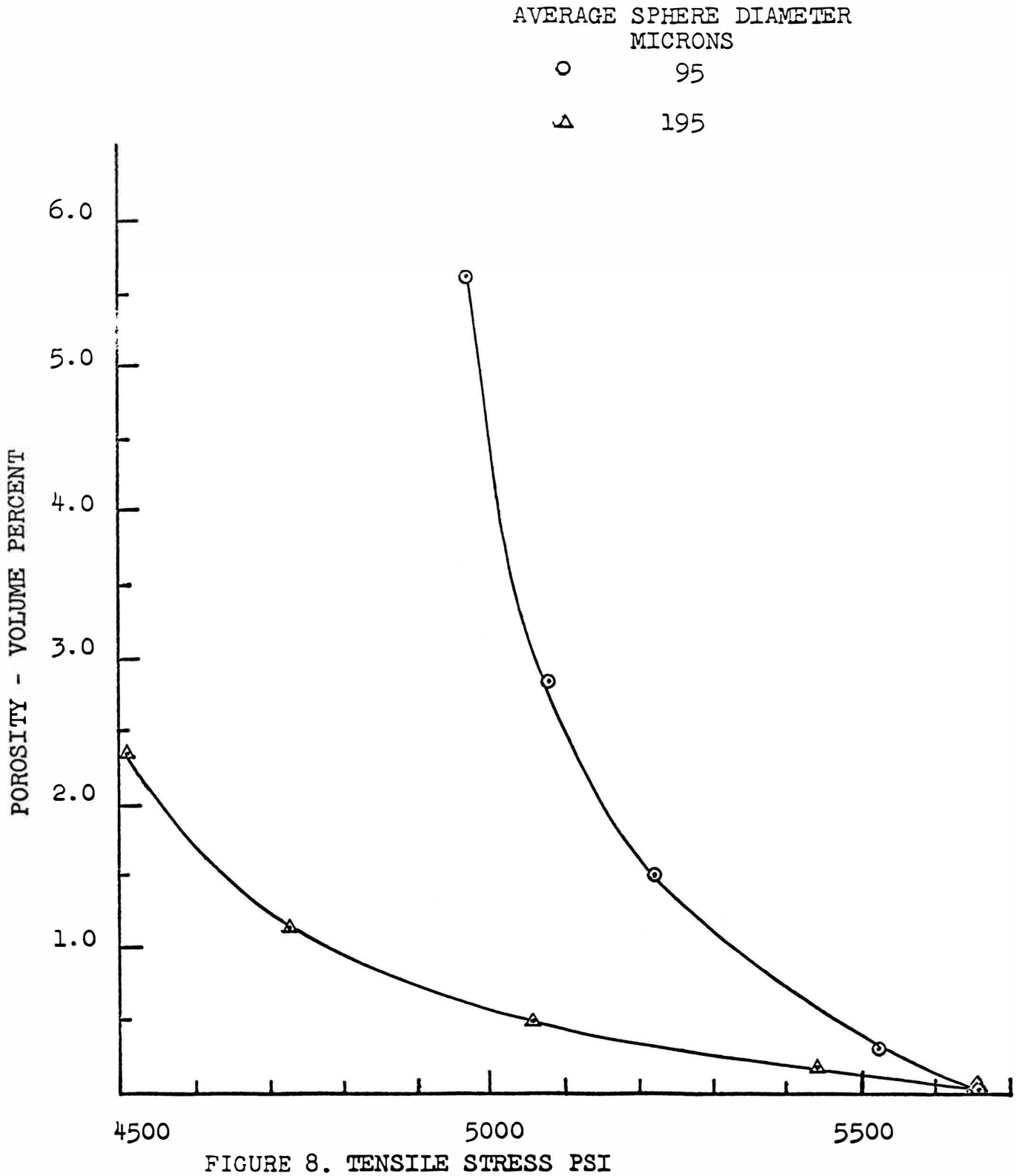


FIGURE 8. TENSILE STRESS PSI

INDUCED SPHERICAL CLOSED PORE POROSITY
VS
TENSILE STRENGTH IN DIAMETRAL LOADING
(SCREENED DATA)

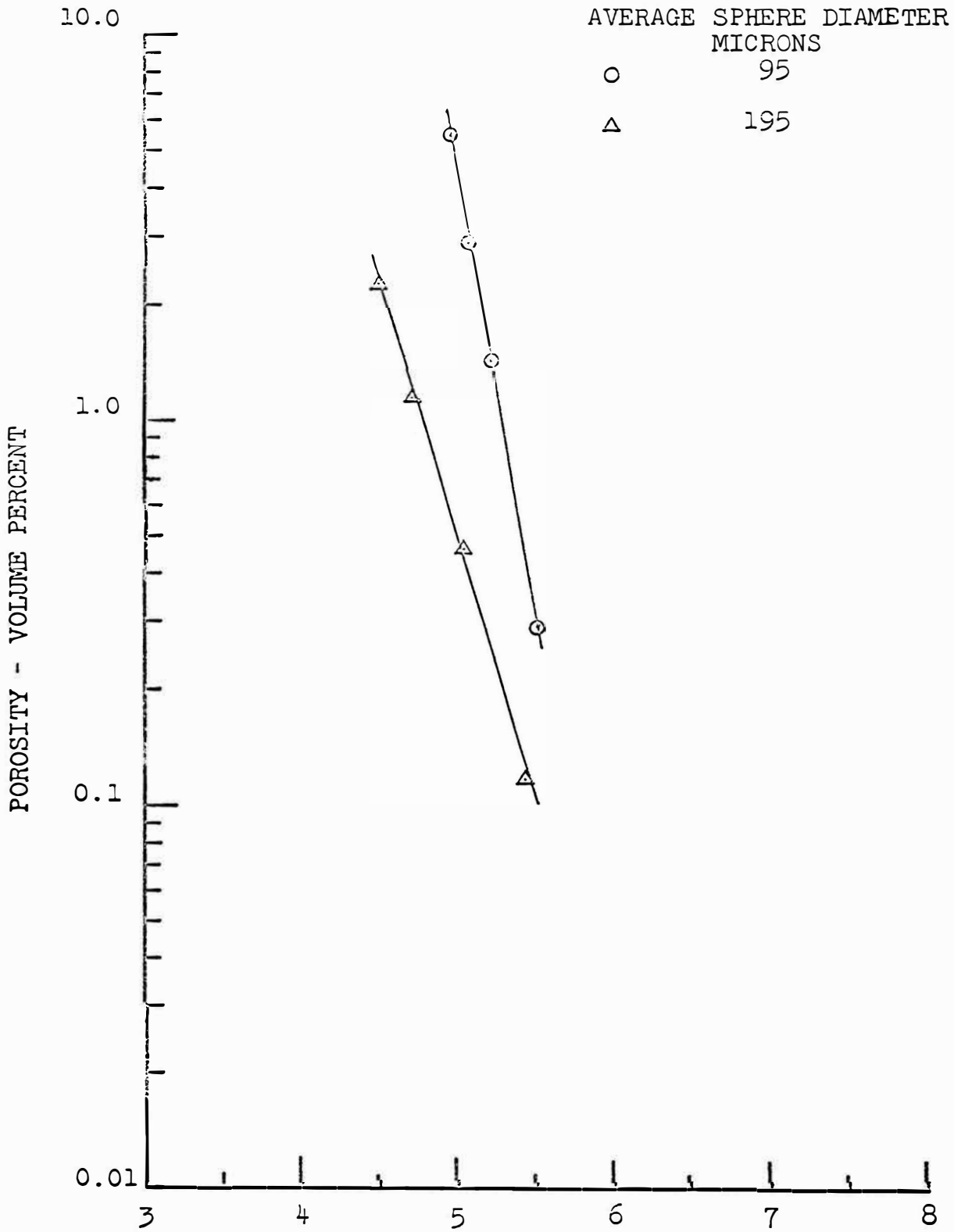


FIGURE 9. TENSILE STRESS PSI X $10^{-3}$

INDUCED SPHERICAL CLOSED PORE POROSITY $p$
VS.
TENSILE STRENGTH IN DIAMETRAL LOADING
(UNSCREENED DATA)

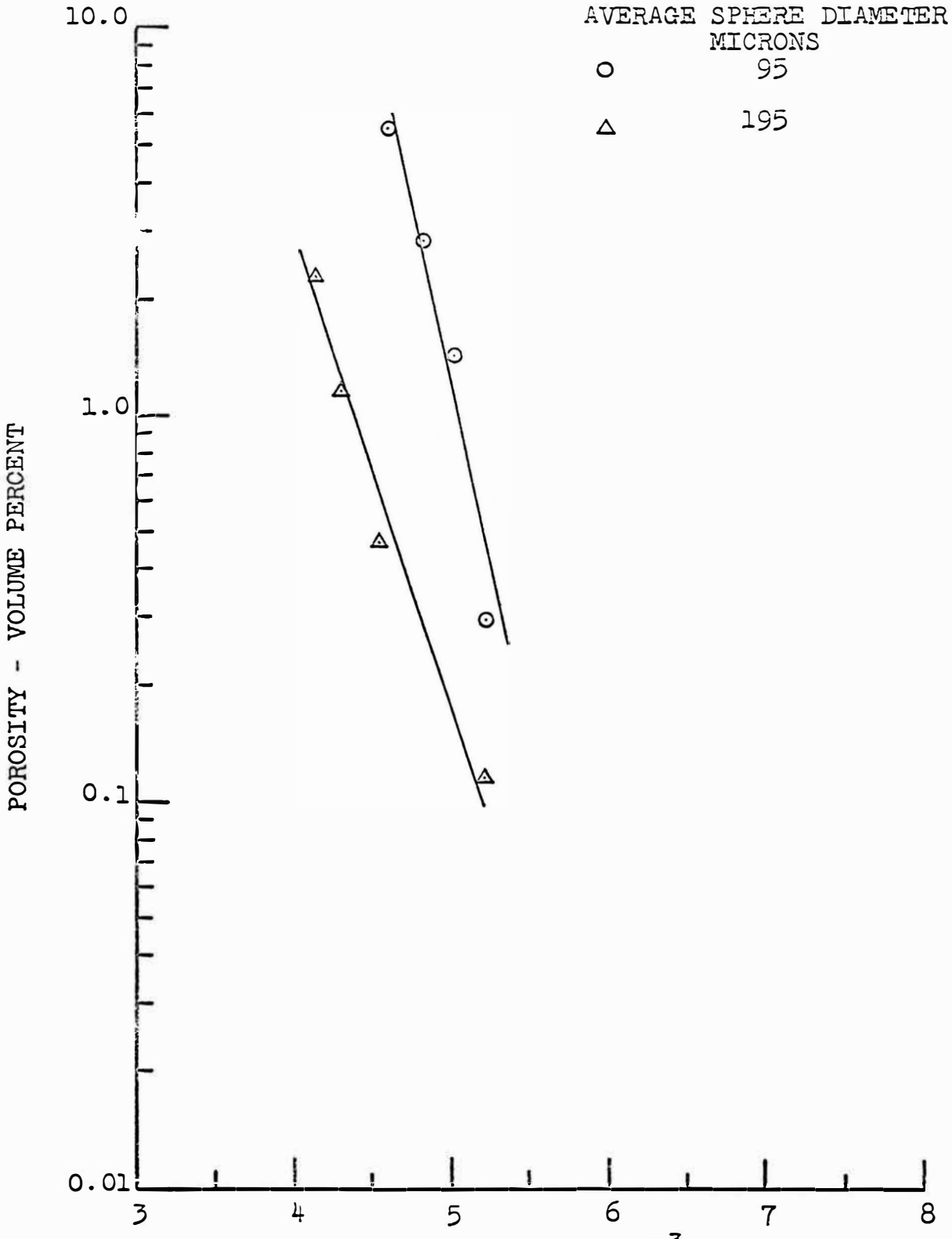


FIGURE 10 TENSILE STRESS PSI X $10^{-3}$

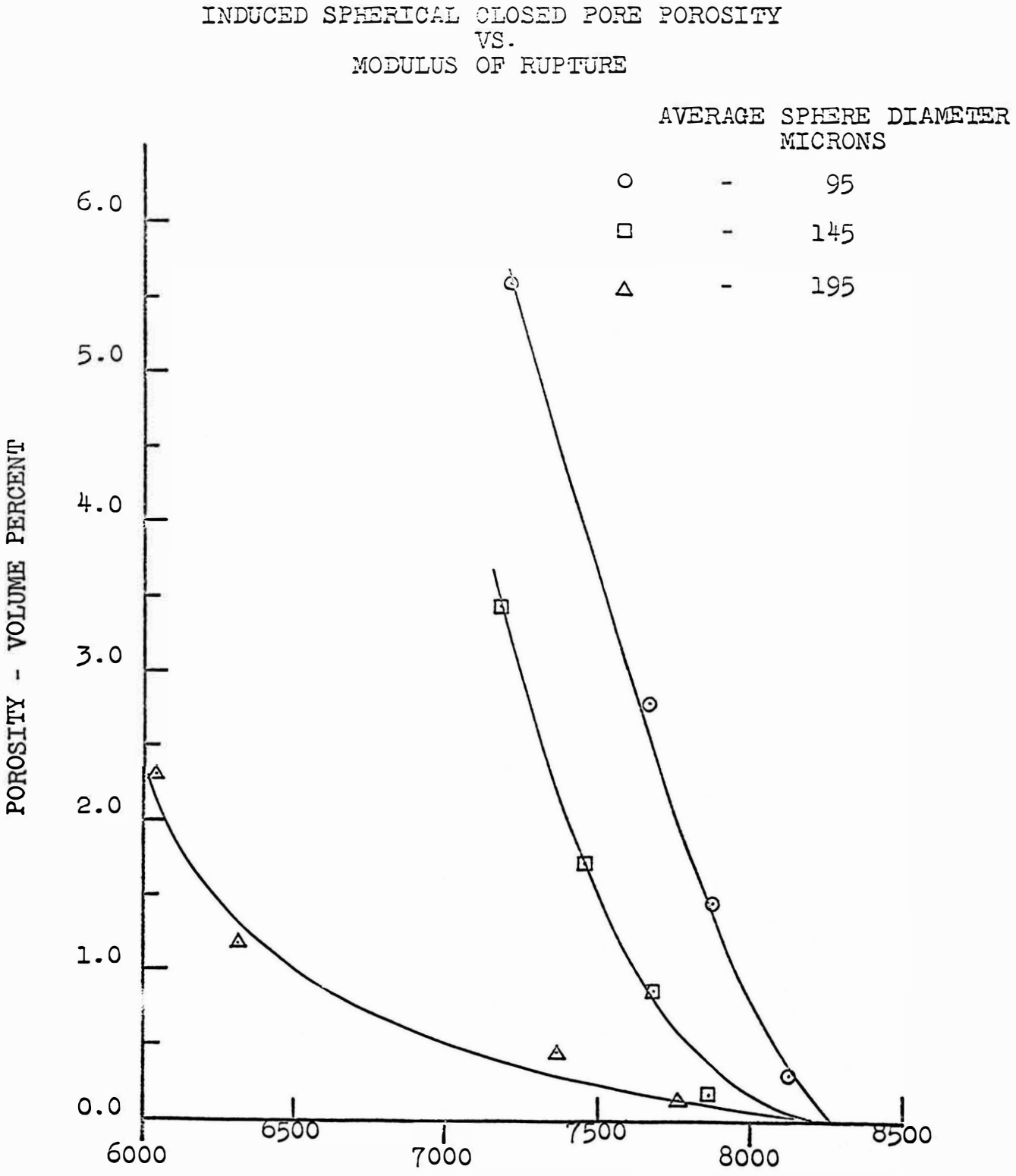


FIGURE 11. FIRED MODULUS OF RUPTURE PSI

be attributed to different stress distributions of each test. The mode of fracture of the Modulus of Rupture test is principally indicative of the specimen surface. This results from stress distributions or gradients of the bending test which involves maximum stresses at the outer fibers. The outer fiber regions then reflect surface characteristics which derive from methods of formulation, fabrication and firing of the specimens and thus are not representative of the internal microstructure. The linear relationship of Modulus of Rupture versus porosity with a steep curve slope for the 95 micron sphere size shows that the outer fiber surface of the specimen is not nearly as sensitive to the 95 micron sphere additions as it is to the 145 and 195 micron sphere size.

The diametral test, however, will be more indicative of internal microstructure effects than the bending test because fracture initiates internally therefore excluding surface effects. The standard errors of data sets equal to $\sigma/\sqrt{n}$ are given in Table XXXIII for the diametral test fracture stresses for both the screened and unscreened data.

Assuming fracture stresses to be normally distributed 95% of the value should be in the range of plus or minus 2X standard error.

TABLE XXXIII

STANDARD ERROR

SCREENED AND UNSCREENED DATA

FOR DIAMETRAL COMPRESSION

SCREENED DATA

| A-Control-71.9psi | | B-Control-54.3psi | | C-Control-67.4psi | |
|---|---|---|---|---|---|
| A-1 | 60.2 | B-1 | 63.1 | C-1 | 67.4 |
| A-2 | 67.5 | B-2 | 71.5 | C-2 | 77.3 |
| A-3 | 72.9 | B-3 | 86.1 | C-3 | 76.1 |
| A-4 | 59.4 | B-4 | 67.2 | C-4 | 90.5 |

UNSCREENED DATA

| A-Control-81.3psi | | B-Control-76.5psi | | C-Control-76.5psi | |
|---|---|---|---|---|---|
| A-1 | 67.8 | B-1 | 58.6 | C-1 | 57.6 |
| A-2 | 63.3 | B-2 | 74.7 | C-2 | 75.6 |
| A-3 | 82.1 | B-3 | 81.0 | C-3 | 67.9 |
| A-4 | 73.9 | B-4 | 87.2 | C-4 | 80.6 |

C. Fracture Stresses as a Function of Quartz Grain Concentration

Experimental work has been conducted by Weyand[23] which relates fracture stresses in diametral loading versus quartz grain concentration in an alumina porcelain. The graphical results are shown in Figures 12 and 13. The separation of the screened data from the unscreened data involves the same methos as described previously. This data plotted straight lines on semi-logarithmic paper; i.e. log quartz concentration is linearly related to mean fracture stress.

As shown by Figures 12 and 13 the slope of the 80-100 mesh quartz particle addition is greater than the 200-230 or 140-170 mesh particles. The slopes of the sphere additions are much steeper than those of the quartz additions but a direct correlation cannot be made between induced porosity and weight percent of quartz. The general trend for both of these is nearly the same.

This type of dependency of fracture strength on low concentrations of an induced phase has been observed by Palmour[24] and Wilkonson[25].

Palmour doped spinel specimens with graphite in concentrations between 0.001 to 10 weight percent. The graphite particles were lens shaped and caused a marked decrease in strength which followed a semi-logarithmic relationship as found in this study.

WEIGHT PERCENT OF ROUNDED QUARTZ
VS.
TENSILE STRENGTH IN DIAMETRAL LOADING
(SCREENED DATA)

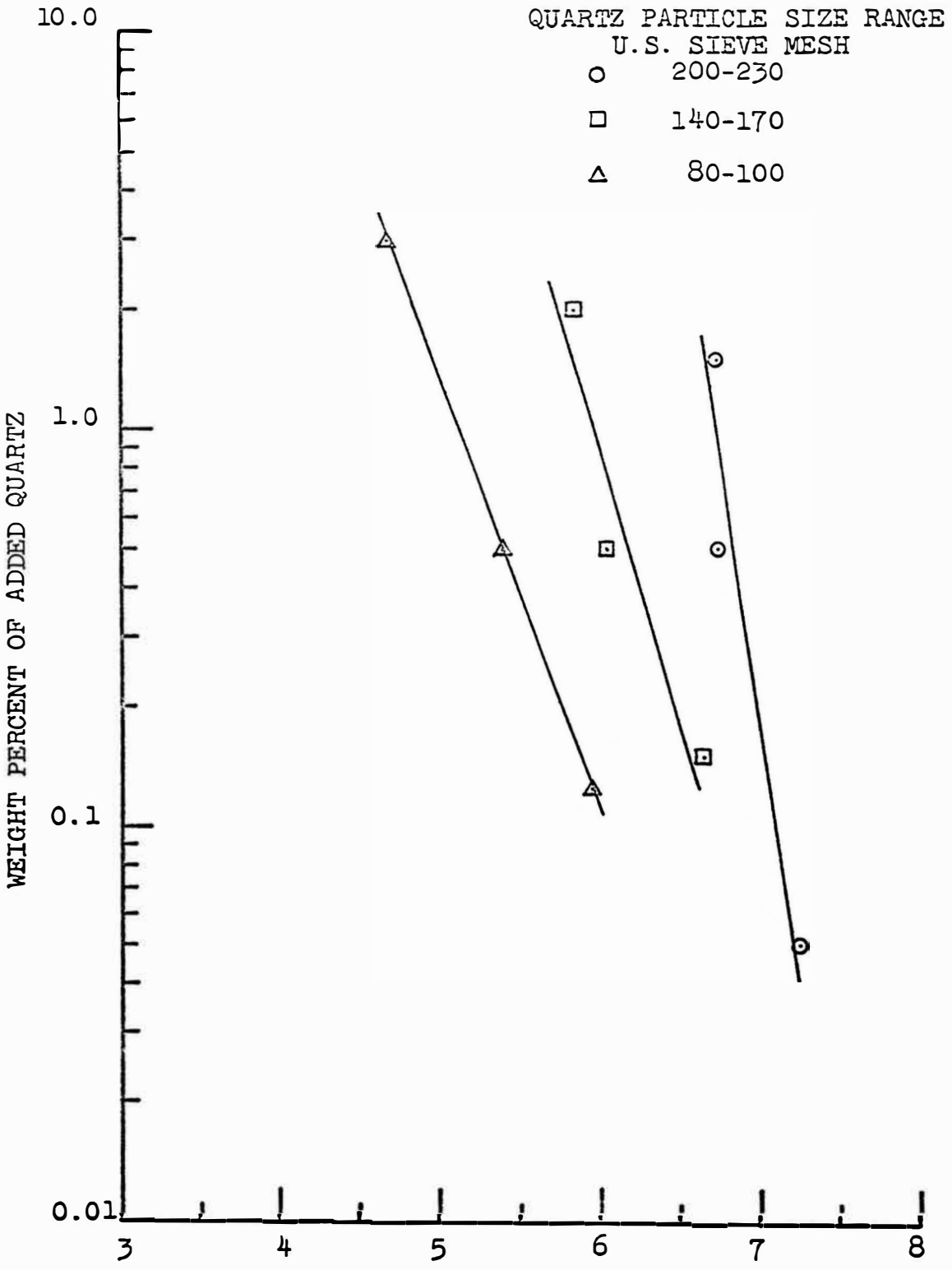


FIGURE 12. TENSILE STRESS PSI X $10^{-3}$

WEIGHT PERCENT OF ROUNDED QUARTZ
VS.
TENSILE STRENGTH IN DIAMETRAL LOADING
(UNSCREENED DATA)

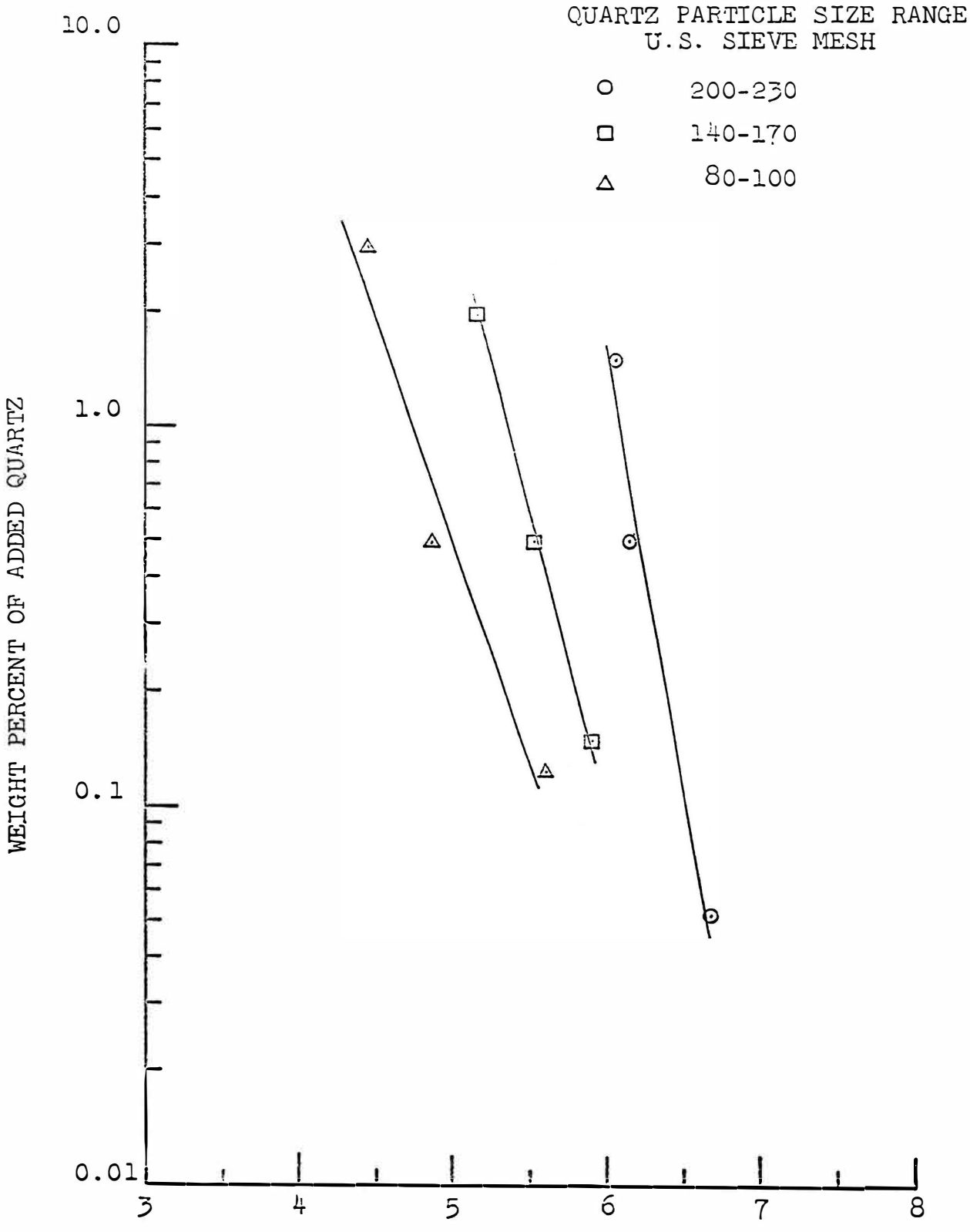


FIGURE 13. TENSILE STRESS PSI X $10^{-3}$

Wilkonson noted a similar effect of inclusion size in studies of strength in bending as a function of the quartz particle size. He found that the strength reduction increased rapidly in the range of 100 to 200 micron diameter particle.

Fracture stresses in porcelain with induced porosities of 0.10 to 7.0 volume percent are described by the semi-logarithmic relationship of log porosity versus fracture stress. The assumption that has been made previously, implies that the interaction between flaws has been minimized. This assumption is not completely valid. Strengths reported by Ryshkewitch[9] in materials with porosities in the range from 3 to 62% are described by a log strength versus porosity relation. Since his percent volume induced porosity is large, interactions between pores to form very serious flaws is a possible explanation for Ryshkewitch's results. His percent volume porosities were of the range in which coincident pores could not be avoided.

The equation suggested by Duckworth[10] describes Ryshkewitch's data. This suggests then that the strength-porosity relationship is a log porosity function for small concentrations and when coincidence of pores occur to form more serious flaws or an interconnecting network of the pore phase the log strength relation is applicable.

Observing the change of slopes for the diametral fracture data in Figure 8 the smaller bead size approaches a linear curve as the concentration of voids increase. The fracture stresses of specimens with small concentrations of the 95 micron bead size then becomes linear as porosity increases. This indicates that a smaller pore size would give a linear plot for porosity versus fracture stress. If the strength of the procelain was increased by removing some of the tramp quartz particles then possibly pores sizes of less than 95 microns would still display a linear relation between log porosity and fracture stress. The stronger materials will be highly sensitive to induced flaws so the minimum size flaw that obeys the semi-logarithmic relationship will decrease with an increasing inherent body strength.

As previously stated the results of this investigation indicate a linear relation between log porosity and mean fracture stress for electrical porcelain. At present there is not an indication of the effect of higher concentrations of (10 to 60%) pores in the size range of 95 to 200 microns, but one would suspect the Ryshkewitch relationship to be valid in this range. The relationship probably extrapolates linearly back to zero porosity for small size pores as indicated by the diametral fracture stresses as a function of porosity which become more linear as pore size decreases (See Figure 8). This investigation shows the effect of pore shape and size.

# CHAPTER VI

# CONCLUSIONS

The conclusions which may be drawn from the result of the work are listed as follows:

1) When spherical pores of 95-200 microns are induced in electrical porcelain, the fracture stresses obtained by the diametral loading method are related to log porosity by a linear plot.

2) It is thought that an induced spherical pore acts as a stress riser or flaw inducer to concentrate stresses or induce serious flaws of sufficient magnitude to initiate failure of the weakest flaw in close proximity with the pore.

3) When the concentration of pores acting possibly as stress risers or flaws is increased the fracture stresses of electrical porcelain should decrease and a concentration should be reached at which the interaction of stress risers and/or flaws cause the strength to be severely decreased.

4) When low concentrations of quartz particles are induced in electrical poreclain a semi-logarithmic plot similar to that of log porosity versus strength is found.

5) The logarithmic relationship does not occur in bending until a pore size of 95 to 145 microns is

present. This indicates the surfaces of the specimens fabricated in this investigation were not sensitive to induced pore sizes below 95 microns.

6) The diametral loading method is more sensitive to 95 micron sized pores than the bending test. This is due to the larger volume of material which is stressed and to the biaxial stresses during testing.

7) It is possible that the pore size effect is related to the intrinsic strength of the material.

# SUGGESTIONS FOR FURTHER STUDY

The present investigation should be extended to higher pore concentrations to observe the change in fracture stress and determine whether the semi-logarithemic relation between log porosity versus fracture stress changes to the Ryshke-witch[9] relation or one of similar nature.

# BIBLIOGRAPHY

1. Moore, R. E., Statistical Analysis of Fracture Stresses of Triaxial Porcelain Bodies, Ph.D. Dissertation, University of Missouri, Columbia, Mo., June 1962

2. Coble, R. L. and Kingery, W. D., Effect of Porosity on Thermal Stress Fracture, Jour. Amer. Cer. Soc. 38 33 (1955)

3. Cutler, Ivan B., Strength of Sintered Alumina in Relation to Porosity and Grain Size, Jour. Amer. Cer. Soc. 40 20-23 (1957)

4. Manson, S. S. and Smith, R. W., Theory of Thermal Shock Resistance of Brittle Materials Based on Weibull's Statistical Theory of Strength, Jour. Amer. Cer. Soc. 38 18 (1955)

5. Weibull, W., A Statistical Theory of the Strength of Materials, Ing. Vetenskaps Akad. Handl. No. 151, 1-45 (1939)

6. Russell,H. W., Principles of Heat Flow in Porous Insulators, Jour. Amer. Cer. Soc. 18 1 (1935)

7. Burke, J. E., Role of Grain Boundaries in Sintering, Jour. Amer. Cer. Soc. 40 80 (1957)

8. Seigle, L., Role of Grain Boundaries in Sintering, Kinetics of High Temperature Processes, p. 173 M.I.T. Press and John Wiley and Sons, 1959 London

9. Ryshkewitch, E., Compression Strength of Porous Sintered Alumina and Zirconia. 9th Communication to

Ceramography, Jour. Amer. Cer. Soc. 36 65 (1953)

10. Duckworth, W., Discussion of Ryshkewitch Paper 36 68 (1953) See Reference 9 for paper under discussion.

11. Cutler, Ivan B., Strength Properties of Sintered Alumina in Relation to Porosity and Grain Size, Jour. Amer. Cer. Soc. 40 20-23 (1957)

12. Knudsen, F. P., Dependence of Mechanical Strength of Brittle Polycrystalline Specimens on Porosity and Grain Size, Jour. Amer. Cer. Soc. 42 377 (1959)

13. Duwez, P. and Martens, H. E., Powder Metallurgy of Porous Metals and Alloys Having Controlled Porosity, Trans. Am. Inst. Mining and Met. Engrs., Inst. of Metals Div. 175 (12) 848-74 (1948)

14. Squire, A., Density Relationships in Iron-Powder Compacts, Trans. Am. Inst. Mining Met. Engrs., Inst. Metals Div. 171 (9) 485-503 (1947)

15. Spriggs, R. M., Expression for Effect of Porosity on Elastic Modulus of Polycrystalline Refractory Materials, Particularly Aluminum Oxide, Jour. Amer. Cer. Soc. 44 628-29 (1961)

16. Knudsen, F. P., Effect of Porosity on Youngs Modulus of Alumina, Jour. Amer. Cer. Soc. 45 91-95 (1962)

17. Hasselman, D. P. H., On the Porosity Dependence of the Elastic Moduli of Polycrystalline Refractory Materials, Jour. Amer. Cer. Soc. 45 452-453 (1962)

18. Spriggs, R. M., Effect of Open and Closed Pores on Elastic Moduli of Polycrystalline Alumina, Jour.

Amer. Cer. Soc. 45 454 (1962)

19. Cutler, Ivan B., The Influence of Impurities on the Brittle Fracture of Inorganic, Non-Metallic Ceramics, Tech. Doc. Report. No. ASD-TR-61-628 Task 8 Armour Research Foundation of I.I.T. Chicago, Illinois, April, 1962

20. Carneiro, P., A New Method for Determination of the Tensile Strength of Concrete, Paris Reuniondes Laboratories d'Essai de Materiaux, June 1947

21. Wright, P. J., Comments on an Indirect Tensile Test on Concrete Cylinders, Mag. Concrete Res. 7 87-96 (1955)

22. Rudnick, A., Hunter, A. R., Holden, F. C., An Analysis of Diametral-Compression Test. Materials Research and Standards, April, 1962.

23. Weyand, John, Unpublished data for Masters thesis, Missouri School of Mines and Metallurgy, Rolla, Missouri to be finished September 1963

24. Palmour, H., Slip Processes in Fine-Grained Polycrystalline Spinel, Mg $Al_2O_4$ Tech. Report No. 1 ARO (D) Project No. 2918-MC Contract Number DA-11-009-ORD-903

25. Wilkonson, W. T. and Dinsdate, A., Spit-Out, Trans. Brit. Cer. Soc. 60 33-66 (1961)

# APPENDIX A

# DERIVATION OF STRESSES IN A DIAMETRALLY LOADED CYLINDER

## Introduction

A new test has been introduced by Fernando Carneiro of Brazil, in which a compressive load is applied to a cylinder along two opposite generators. This conditions sets up a uniform tensile stress over the diametral plane containing the applied load, and fracture occurs along this plane. The test is carried out in a compression testing machine, strips of packing material normally being placed between the specimen and the platens of the machine. An attractive feature of the test is that it enables similar specimens, and the same testing machine, to be used for both tensile and compressive strength tests.

## The Distribution of Stress in a Diametrally Loaded Disc

It has been shown by mathematical analysis that a compressive load applied perpendicularly to the axis of a cylinder and in a diametral plane gives rise to a uniform tensile stress over that plane. A simplified treatment of this problem as described by Frocht is given below. The theory is based on two fundamental conditions of stress distribution, which can both be deduced by mathematical analysis.

The first basic stress distribution is that due to a concentrated force p (Figure 14) acting on the edge of a

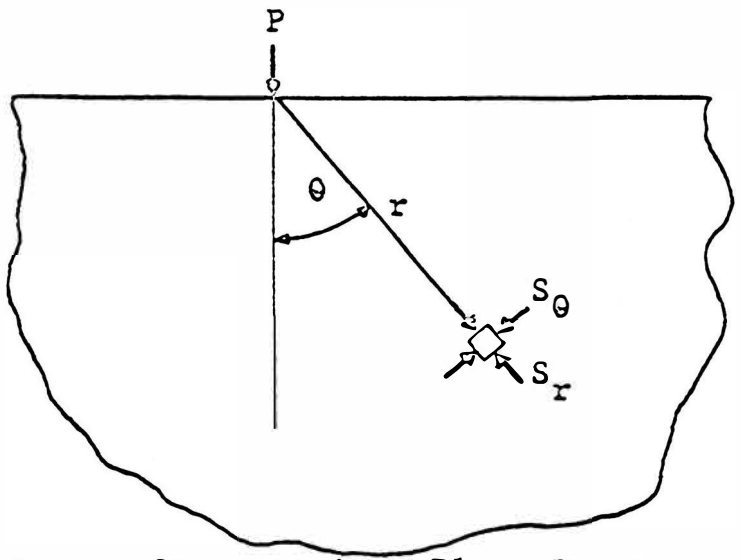


Figure 14. Stresses in a Plate Due to a Concentrated Load Applied to an Edge.

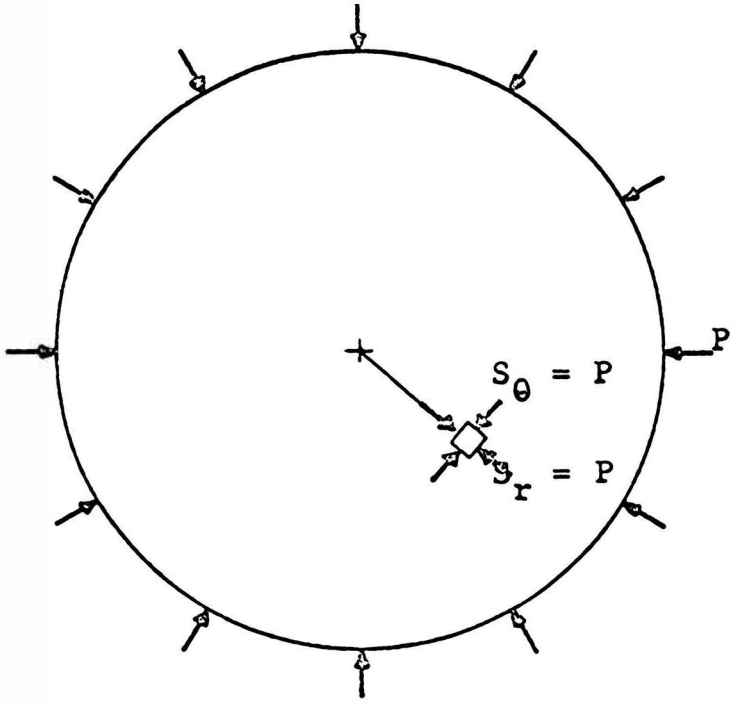


Figure 15. Stresses in a Disc Due to a Uniform Radial Pressure P.

plate of thickness t bounded by one Straight edge but otherwise unlimited in extent. Assuming the material to obey Hooke's law that stress is proportional to strain, and assuming a condition of plane stress (i.e. no stresses perpendicular to the plane of the plate), the stress components on the element shown are:

| | |
|---|---|
| radial stress, towards the point of application of the load | $S_r = \frac{2P}{\pi t} \frac{\cos \theta}{r}$ |
| circumferential stress, perpendicular to $S_r$ | $S_\theta = 0$ |
| shear stress | $t_{r\theta} = 0$ |

Thus a concentrated load gives rise to a radial compression which decreases as r increases and as $\theta$ increases.

The second basic stress distribution is that in a circular disc subjected to a uniform pressure P round the edge (Figure 15). Making the same assumptions as previously, the stress in any direction and at any point is equal to the applied pressure P, and there is no shear.

$$S_r = P$$

$$S_\theta = P$$

$$t_{r\theta} = 0$$

In Figure 16 is shown a circular disc subjected to a concentrated load P, the disc being considered as part of the plate in Figure 14. At any point on the circumference there is a stress $\frac{2P}{\pi t} \frac{\cos \theta}{r}$ acting towards O, and, from the

Figure 16. Stress at the Circumference of a Circular Area of the Plate Shown in Figure 14.

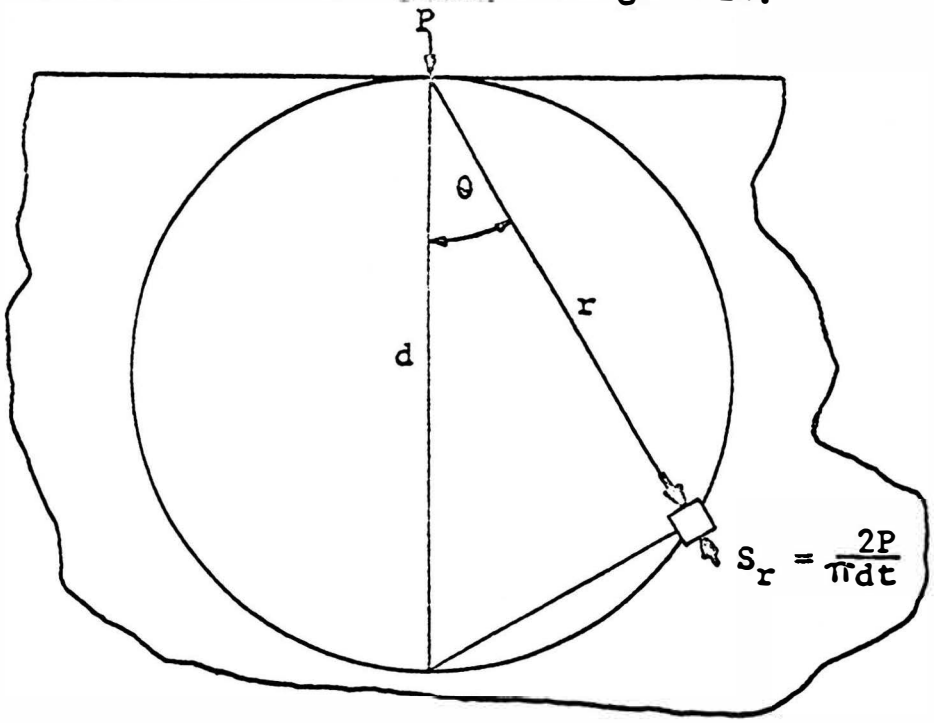


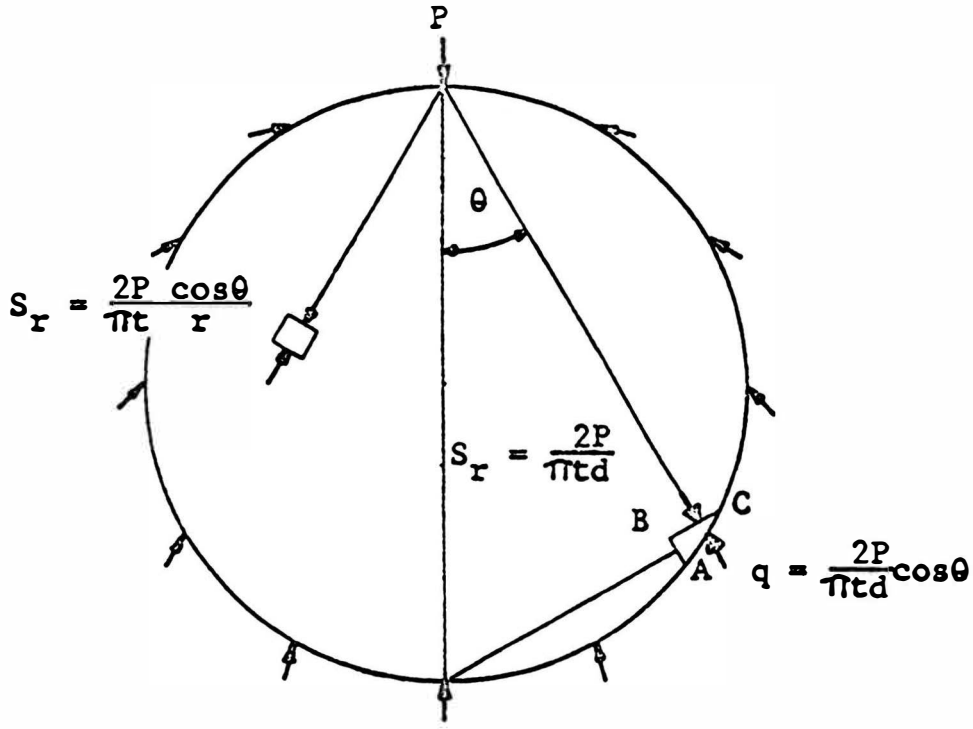


Figure 17. A Disc Subjected to the Same Loading as the Circular Area of the Plate in Figure 16.

geometry of the figure, $r/d = \cos \theta$. Therefore

$$S_r = \frac{2P}{\pi t} \frac{1}{d}$$

Let the circular area be removed from the plate (Figure 17) and such stresses, q, be applied to the circumference as will maintain the same conditions of stress within the disc; i.e, let stresses be applied exactly equal to those exerted by the surrounding area of the plate. Considering the equilibrium of the element ABC,

$$\frac{2P}{\pi td} BC = qAC$$

Therefore

$$q = \frac{2P}{\pi td} \frac{BC}{AC} = \frac{2P}{\pi td} \cos \theta$$

There are no forces in the direction BC. The stress at any point within the disc is still

$$\frac{2P}{\pi t} \frac{\cos \theta}{r}$$

The conditions would be similar, if the force P acted on the bottom of the disc, and, therefore, upon the system of stresses already described, a similar inverted system may be superimposed (Figure 18). We now have a disc subjected to two opposite forces P acting along a diameter, and two sets of stresses, acting on the circumference, of magnitude $\frac{2P}{\pi td} \cdot \frac{r}{d}$ along AO and $\frac{2P}{\pi td} \cdot \frac{r_1}{d}$ along $AO_1$. These two external stresses are proportional to AO and $AO_1$ and may therefore be represented by these lines in a parallelogram of stresses. The resultant is clearly $AB = \frac{2P}{\pi td}$, which is constant and passes through the center. Thus the

Figure 18. Two Sets of Forces Superimposed.

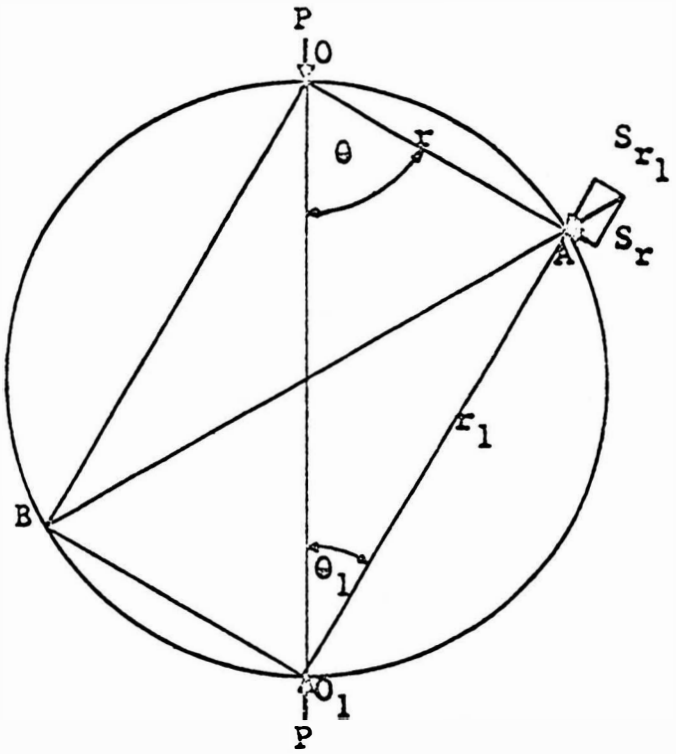


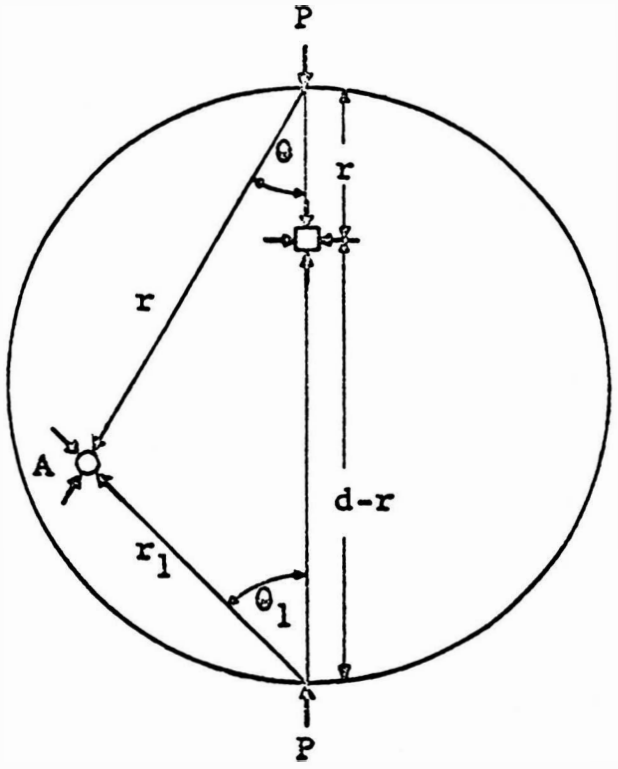


Figure 19. Disc Subjected to Two Concentrated Forces Only.

two systems together are equivalent to a uniform radial compression of magnitude $\frac{2P}{\pi td}$. Any element within the disc is now subject to two radial stresses.

Let us now superimpose a uniform radial tension of magnitude $\frac{2P}{\pi td}$ acting on the circumference of the disc. The resultant distributed loads now vanish, and we are left with the conditions of the problem; i.e. a disc subjected to two opposite forces acting along a diameter (Figure 19). Also, this uniform tension gives rise to a tensile stress $\frac{2P}{\pi td}$ at all points in the disc and in any direction. Any element, A, is therefore subject to the two compressive stress components $\frac{2P}{\pi t} \frac{\cos \theta}{r}$ and $\frac{2P}{\pi t} \frac{\cos \theta}{r_1}$, as indicated, and a tensile stress $\frac{2P}{\pi td}$ in all directions. The exact stresses at any point can thus be calculated readily. In particular, on the vertical diameter,

$$\theta = \theta_1 = 0$$

Thus the vertical stress component (compressive)

$$= \frac{2P}{\pi t} \frac{1}{r} + \frac{2P}{\pi t} \cdot \frac{1}{d-r} - \frac{2P}{\pi td}$$

$$= \frac{2P}{\pi td} \left( \frac{d}{r} + \frac{d}{d-r} - 1 \right)$$

and the horizontal stress component (tensile)

$$= \frac{2P}{\pi td}$$

By considering a cylinder of concrete as a number of such discs, we see that a uniform tensile stress is developed over the vertical diametral plane, and the value of this stress is $\frac{2}{\pi} \frac{P}{DL}$, where D and L are the diameter and length of the cylinder.

# APPENDIX B

## ESTIMATION OF TOTAL ERROR IN CALCULATED INDIVIDUAL FRACTURE STRESSES

The estimate of total error in individual results was determined using a method recommended by Woodman.* The errors in S, the fracture stress are due to errors in assigning numbers to P, the load, D, the diameter, and L, the specimen length, which are related by:

$$S = \frac{2P}{\pi DL}$$

$$\pm\Delta E \text{ (total error)} = \left[ \left(\frac{\partial E}{\partial P}\delta P_1\right)^2 + \left(\frac{\partial E}{\partial D}\delta D_1\right)^2 + \left(\frac{\partial E}{\partial L}\delta L_1\right)^2 \right]^{\frac{1}{2}}$$

for this calculation:

$P_1$ = precision to which P is measured = $\pm$ 25 psi

$D_1$ = precision to which D is measured = $\pm$ 0.0005

$L_1$ = precision to which L is measured = $\pm$ 0.0005

Thus:

$$\pm\Delta E = \left[ \left(\frac{2 \times 25}{\pi DL}\right)^2 + \left(\frac{2P \times 0.0005}{\pi D^2 L}\right)^2 + \left(\frac{2P \times 0.0005}{\pi DL^2}\right)^2 \right]^{\frac{1}{2}}$$

The cylindrical dimensions were nearly constant throughout the tests with $D \approx 0.620$ and $L \approx 0.730$. The value of P ranged from about 3095 to 6695 psi; consequently the total error varied as well. For these extreme values of P, $\pm\Delta E$ varied from 35.0to 36.4 psi.

---

*Woodman, L. E., "Application of Theory of Measurements to Certain Engineering Problems," Univ. Missouri School of Mines and Metallurgy Bulletin., Tech. Series, 15 (1952).

To facilitate the construction of frequency distribution tables, it was decided to round off calculated values of mean fracture stresses to the nearest 50 psi.

# VITA

Edward Anton Snajdr was born November 4, 1938 in Granite City, Illinois. He attended the Edwardsville, Illinois public elementary and high school graduating from the latter in May 1956.

The following September he enrolled in the Missouri School of Mines pursuing course work in Ceramic Engineering. He received the Bachelor of Science in Ceramic Engineering on May 1961.

The following September he enrolled at the Missouri School of Mines pursuing course work leading to a Master of Science in Ceramic Engineering. On June 2, 1962 he was married to Miss Sally Ann Bartlett of Berkeley, Missouri.

He has been employed by A. P. Green Firebrick Company of Mexico Missouri and Alton Brick Company of Alton, Ill.